R. & M. No. 3434

MINISTRY OF AVIATION

AERONAUTICAL RESEARCH COUNCIL
REPORTS AND MEMORANDA

On the Prediction of Base Pressure in Two-Dimensional Supersonic Turbulent Flow

By J. B. Roberts

LONDON: HER MAJESTY'S STATIONERY OFFICE
1966
PRICE £1 3*s.* 0*d.* NET

On the Prediction of Base Pressure in Two-Dimensional Supersonic Turbulent Flow

By J. B. Roberts

Communicated by the Deputy Controller Aircraft (Research and Development), Ministry of Aviation

*Reports and Memoranda No. 3434**

November, 1964

Summary

The theory of base-pressure prediction in two-dimensional supersonic turbulent flow is discussed, and, in the light of recent investigations of jet mixing, various modifications to the analysis of the flow model are suggested. A comparison is made of some reattachment criteria, and a Mach number ratio is proposed as a simple criterion, which correlates the experimental data satisfactorily.

LIST OF CONTENTS

* Replaces N.G.T.E. Report No. R.265—A.R.C. 26 720.

LIST OF TABLES

LIST OF APPENDICES

LIST OF ILLUSTRATIONS

---

1. *Introduction.*

Recent proposals for supersonic transport aircraft have led to considerable interest in methods of predicting the base pressure associated with the engine installations of such aircraft. Since the flow mechanisms involved in practical problems of this nature are complex and little understood, investigations of base-pressure phenomena are usually confined to simpler flow models, in the hope that some fundamental knowledge will be obtained, capable of general application.

The simplest types of base flow model are the two-dimensional backward-facing step and the blunt trailing-edge wing, both having many features in common. It has been shown theoretically by Crocco and Lees[1], and demonstrated experimentally, that the base pressure associated with these simple flow models can be influenced to a great extent by the existence and location of transition from laminar to turbulent flow. Here, the case will be considered where the flow is everywhere turbulent, and the analysis will be limited to conditions where the external flow is supersonic.

Chapman[2] and Korst[3] have independently proposed a simple analysis which may be used to predict base pressure. The essence of this treatment lies in the assumption that the flow model may be split into a number of components, each of which is analysed separately. The results may then be combined to give a picture of the complete flow pattern.

Figure 1 shows the flow pattern for a backward-facing step. A uniform stream with a turbulent boundary layer approaches the step and separates at the corner. The free stream turns through the appropriate Prandtl-Meyer angle, and the boundary layer develops into a free shear layer in a region of effectively constant base pressure. As the shear layer approaches the downstream wall it is compressed, and part of the shear layer reverses into the slowly circulating fluid within the base cavity, whilst the remainder negotiates the pressure rise and forms a new uniform stream, with a re-developed boundary layer, some distance downstream of the step. The equivalent flow pattern for a blunt trailing-edge wing is similar, although here the recompression of the shear layer is due to the convergence of symmetrical shear layers on either side of the wing, and clearly a new boundary layer will not be formed downstream of the recompression zone in this case.

Chapman[2] and Korst[3] have supposed that a particular streamline (the 'dividing' or 'reattachment' streamline) could be specified, that would divide the recirculating flow from the rest, and would be the only streamline to stagnate completely. By considering the mixing process in the shear layer to be independent of any recompression effects, they were able to compute the velocity on the reattachment streamline, from a knowledge of the velocity distribution in the shear layer, and by considering the conditions for mass continuity within the wake.

For a prediction of base pressure, it was found necessary to supply a further piece of information about the 'reattachment' streamline. These same authors proposed the 'escape' criterion, which states that the stagnation pressure of the reattachment streamline, assuming it to compress isentropically, can be equated to the static pressure in the uniform region downstream of the reattachment zone. This, in effect, assumes that only streamlines with a total pressure greater than the downstream static pressure are capable of overcoming the pressure rise at reattachment, and 'escaping' from the cavity.

By use of this criterion, Korst[3] was able to predict the base pressure in supersonic turbulent flow, for the particular case of no initial boundary layer. This theory was found to agree quite well with a large body of experimental data, where the initial boundary-layer thickness was small.

Recently, Nash[4] has examined the effect of the initial boundary layer, by using a simple approximation proposed by Kirk[5]. He has shown that when the boundary layer is properly accounted for, Korst's theory leads to incorrect base-pressure predictions. By assuming that the reattachment streamline stagnates to the local pressure at the reattachment point, instead of the downstream static pressure, the discrepancy between theory and experiment was removed, and at the same time the flow model used for analysis was made physically more acceptable.

The problem remained of relating the pressure at the reattachment point to that downstream of the recompression zone. Nash[4] proposed a factor N which defined the ratio in which the reattachment pressure divided the total pressure rise, and suggested that this factor was about $0{\cdot}35$, as opposed to the value of $1{\cdot}00$ used by Korst. McDonald[6] has pointed out that use of this factor N is not completely satisfactory, since it depends to some extent on Reynolds number and Mach number. By considering the recompression of the shear layer to be isentropic, McDonald was able to compute the shape parameter of the boundary layer at the reattachment point, and from a modification of the relationship derived by Reshotko and Tucker[7], he produced a method for determining the shape parameter of the re-developed boundary layer. From a comparison of some experimental results, he concluded that the final shape parameter of the equivalent, incompressible boundary layer was about $1{\cdot}4$, and has suggested that this value should be used as a reattachment criterion.

In the present report, a theoretical treatment of the conventional flow model will be given, containing some significant differences of detail. Available experimental data will be analysed, and used to assess the validity of various reattachment criteria, including those of Nash and McDonald.

2. *Flow-Model Analysis.*

It has already been mentioned that the analytical method relies on the assumption that the flow model shown in Figure 1 can be split into a number of parts, each of which may be considered separately. Starting just upstream of the step and working downstream, it will be seen that the following problems arise:

(i) It is necessary to know the effect of the corner expansion on the velocity profile of the initial boundary layer. The analysis of this problem is discussed in Section 2.1. The expanded boundary layer can be regarded as the initial state from which the shear layer develops.

(ii) The velocity distribution in the shear layer is required. It will be shown that the effect of the expanded boundary layer can be taken into account by considering an 'asymptotic shear layer' to start from a false origin, with zero initial thickness. This approximation enables a simple flow model, discussed in Section 2.2, to be used. An important datum for this shear layer is the 'median

streamline', which has a constant velocity. The method of finding this velocity is considered in Section 2.3. Methods of determining the rate of spread of the shear layer, which is a function of Mach number, are compared in Section 2.4. In Section 2.5, the appropriate analysis for locating the false origin of the asymptotic shear layer is given. The effect of bleed flow may be quite readily incorporated into the analysis, as discussed in Section 2.6.

(iii) To complete the analysis, the manner in which the free shear layer compresses to form a new boundary layer downstream of the base must be considered. In Section 2.7, this problem is discussed in some detail.

2.1. *Abrupt Expansion of the Initial Boundary Layer.*

We shall consider first the expansion process accompanying separation of the flow at a backward-facing step. This is shown diagrammatically in Figure 2.

The velocity profile of the initial boundary layer may be considerably modified as it passes through the expansion fan at separation. In order to estimate the effect of initial boundary-layer thickness on the subsequent development of the shear layer, it is necessary to know the momentum thickness of the boundary layer at the end of this expansion.

Since the expansion is a rapid process, it is reasonable to suppose that viscous forces are negligible in comparison with pressure forces. If it is further assumed that the flow along any streamline through the expansion is isentropic, an analysis may be framed from the one-dimensional isentropic relations.

It is shown in Appendix II that, if the assumptions mentioned above are employed, the resulting analysis yields the expression

$$\frac{\rho_{E,1}u_{E,1}\theta_1}{\rho_{E,0}u_{E,0}\theta_0} = \frac{\displaystyle\int_0^1 \frac{\phi_0^n d\phi_0}{(1-C_{E,0}^2\phi_0^2)} - \int_0^1 \frac{\phi_0^n[KC_{E,0}^2\phi_0^2-(K-1)]^{1/2}}{(1-C_{E,0}^2\phi_0^2)C_{E,0}}\,d\phi_0}{\displaystyle\int_0^1 \frac{\phi_0^n(1-\phi_0)d\phi_0}{(1-C_{E,0}^2\phi_0^2)}} \tag{1}$$

This equation enables θ_1/θ_0 to be determined for particular values of p_1/p_0, $M_{E,0}$ and n. The integral expressions on the right-hand side of the equation must be solved by a numerical method for each case.

In Figure 3 the variation of θ_1/θ_0 with p_1/p_0, as computed by the author from the above equation, is shown for $M_{E,0} = 2$ and $n = 7$. This is compared with the corresponding variation predicted by the methods of Nash[4] and of Carrière and Sirieix[8]. Nash's approximation to equation (1) is

$$\frac{\rho_{E,1}u_{E,1}\theta_1}{\rho_{E,0}u_{E,0}\theta_0} = \frac{M_{E,0}^2}{M_{E,1}^2}.$$

Carrière and Sirieix have computed their results from expressions equivalent to equation (1), although their numerical results differ substantially from those of the author for values of p_1/p_0 between 0·5 and 1·0. It will be observed from Figure 3 that, while Nash's approximation gives the correct trend of θ_1/θ_0 with changing p_1/p_0, it gives values of θ_1/θ_0 which are always too great.

In Figure 4, the variation of θ_1/θ_0 with p_1/p_0 is shown for $M_{E,0} = 2{\cdot}0$, and values of n of 5, 7 and 9, as computed from equation (1). It would appear from these results that θ_1/θ_0 is only slightly dependent on n, for specified values of p_1/p_0 and $M_{E,0}$. In future calculations, therefore, little error can be incurred by assuming that n is always 7.

Figure 5 depicts the variation of the parameter

$$\frac{\rho_{E,1} u_{E,1} \theta_1}{\rho_{E,0} u_{E,0} \theta_0}$$

with p_1/p_0, for values of $M_{E,0}$ of 1·0, 1·5, 2·0, 2·5, 3·0 and 4·0, and Figure 6 gives the corresponding variation of θ_1/θ_0. (n taken to be 7.)

For specified values of p_1/p_0 and $M_{E,0}$, the appropriate value of θ_1/θ_0 may be found quite readily by interpolation from Figure 6.

2.2. *Shear-Layer Velocity Profile.*

The boundary layer separates at the expansion corner and develops into a free-shear layer, which serves to partition the external flow from the slowly circulating fluid in the cavity just downstream of the step. Providing that the velocity of circulation in the cavity is low, the pressure in this region is fairly uniform. Since the recompression region which forms when the shear layer interacts with the downstream wall does not appreciably affect the growth of the shear layer upstream of this region, and since the streamlines in the flow external to the free-shear layer are straight and parallel if the flow is supersonic and two-dimensional, the velocity distribution in the shear layer is thus approximately the same as in a mixing region between air at rest and a supersonic stream. The growth of this mixing region will be affected by the thickness of the initial boundary layer. Here, however, we shall only consider the limiting case of zero initial boundary-layer thickness (the appropriate flow model is then as shown in Figure 7). It will be shown in a later section how a simple correction may be applied to allow for the effect of initial boundary-layer thickness.

The flow model illustrated in Figure 7 has been examined theoretically by a number of authors[9, 10, 11, 12]. It is generally recognised that the velocity at any point in the free-shear layer may be represented in non-dimensional terms by a relationship of the form,

$$\phi = \frac{u}{u_E} = f\left(\frac{\sigma y}{x}\right) \tag{2}$$

where σ is a jet spreading parameter dependent on Mach number. x, y are co-ordinates as indicated in Figure 7.

Tollmien[9] used Prandtl's mixing-length theory[13] to study the incompressible mixing of a two-dimensional jet with a free boundary, and his solution provides non-dimensionalised velocity profiles in the form indicated by equation (2). Some values obtained by this theory are given in Table 1. Tollmien's results were later extended by Abramovitch[11] to cover the case of compressible flow up to the speed of sound. Abramovitch found that compressibility had only a slight effect on the properties of the free jet.

Görtler[10] has made use of Prandtl's concept of a virtual kinematic viscosity[14], and solved the equation of motion by a series method. The exact solution of the first two terms provides an approximate velocity distribution given by the error function,

$$\phi = \frac{u}{u_E} = \tfrac{1}{2}\left(1 + \operatorname{erf}\frac{\sigma y}{x}\right). \tag{3}$$

The complete numerical result is referred to as Görtler's theory; some of the values obtained by this method, along with the error function values, are given in Table 1.

Crane[12] has used Görtler's solution as a starting point for analysing the mixing of streams of compressible fluid. Crane concluded that, due to compensating effects, the form of the velocity profile is essentially unchanged by compressibility. Some values for the velocity distribution in incompressible flow computed by this method, are given in Table 1.

It has usually been assumed that the error-function profile provides a sufficiently good fit to measured velocity profiles over quite a wide range of Mach number, providing that appropriate values of σ are taken, and this solution has been widely used in attempts at predicting base pressure (e.g. References 3, 4, 6 and 8). However, a recent extensive experimental study of this problem by Maydew and Reed[15], working at Mach numbers up to 1·96, had indicated that, whilst the measured velocity profiles agree quite well with Crane's (and also Görtler's) theoretical velocity distribution, they are not adequately fitted by either the error-function profile or Tollmien's theoretical profile. Furthermore, Maydew and Reed found no discernible effect of Mach number for $M < 2$ on the shape of the velocity profile, which is in good agreement with Crane's theoretical results.

In view of this evidence, Crane's incompressible velocity profile will be used in subsequent calculations.

2.3. *Median Velocity Ratio.*

It will be noticed from a consideration of the simple mixing flow model shown in Figure 7, and from the form of the velocity profile relation indicated by equation (2), that radial lines from the corner represent lines of constant velocity. It is clear that one of these constant-velocity lines is parallel to the external flow direction and is therefore a streamline. A knowledge of the velocity ratio (ϕ_M) of this 'median' or 'constant-velocity' streamline is of particular importance in base-pressure theory.

From considerations of continuity of mass and momentum in the free-shear layer, it can easily be shown (e.g. Reference 8) that the median velocity ratio is defined by the relation,

$$\int_{\eta_M}^{+\infty} \frac{\phi \, d\eta}{(1 - C_{E,1}{}^2 \phi^2)} = \int_{-\infty}^{+\infty} \frac{\phi^2 d\eta}{(1 - C_{E,1}{}^2 \phi^2)} \tag{4}$$

where

$$\eta = \frac{\sigma y}{x}$$

and from equation (2)

$$\phi_M = f(\eta_M)$$

or generally

$$\phi = f(\eta)$$

It is apparent from equation (4) that ϕ_M is dependent upon the shape of the velocity profile and upon the external Mach number.

If it is assumed that the velocity profile is invariant with Mach number, as Crane's theory would suggest (*see* Section 3.2), then a particular incompressible velocity profile may be taken in the solution of equation (4), enabling ϕ_M to be determined as a function of Mach number.

In Figure 8, the variation of median velocity ratio (ϕ_M) with Mach number is shown, as computed for the error-function profile and for Crane's incompressible profile. The variation of ϕ_M obtained from the error function has been used by Korst[3] and others in the prediction of base pressure. However, as Nash[4] has pointed out, there is a considerable discrepancy between the median velocity variation computed from these two profiles. At low speeds, for example, the error-function profile

gives a ϕ_M of about 0·615, whilst the more precise method of Crane[12] (and Görtler) gives a value of 0·585. A similar difference is maintained throughout the range of Mach number considered (0 to 6). It is interesting to note that, whilst Tollmien's incompressible velocity profile[9] does not fit the experimental distributions adequately, it does lead to a value of ϕ_M of 0·58 at low speeds, which is in close agreement with the method of Crane (and Görtler).

As already mentioned in Section 3.2, Abramovitch[11] has extended Tollmien's results to cover the Mach number range from zero to unity, and this theory may also be used to predict the variation of ϕ_M with Mach number (*see* Appendix III). The results, which have been extended by the present author up to a Mach number of 3, are shown in Figure 8. The rapid increase of ϕ_M with Mach number given by Abramovitch's method indicates that the velocity profile is strongly dependent on Mach number. This would appear to be in contradiction to the more exact theory of Crane, and to the experimental results of Maydew and Reed, although it is worth remembering that the latter have only verified Crane's results up to a Mach number of 2.

In subsequent calculations, the variation of ϕ_M with Mach number obtained from Crane's profiles will be used, it being understood that for Mach numbers in excess of 2, this variation is very tentative, and will probably need some modification as more experimental evidence becomes available.

In Figure 9, it is shown that a close approximation to the proposed variation of ϕ_M with Mach number, for the range $1{\cdot}5 < M_E < 4{\cdot}0$, is given by the relation

$$\phi_M{}^2 = 0{\cdot}330 + 0{\cdot}0256\, M_E. \tag{5}$$

For comparison, Figure 9 includes the corresponding variation assumed by Nash[4], i.e.

$$\phi_M{}^2 = 0{\cdot}343 + 0{\cdot}0180\, M_E.$$

2.4. *Jet Spreading Parameter.*

The jet spreading parameter (σ) has been measured by a number of workers[15 to 26] at various Mach numbers. These results are shown in Figure 10, where σ/σ^* (σ^* being the incompressible value of the jet spreading parameter, taken to be 11) is plotted against Mach number (M_E). It will be observed that the data exhibit wide scatter, although a definite increase of σ with Mach number is indicated.

Various empirical or semi-empirical equations have been suggested for determining σ. Korst and Tripp[27], on the basis of some rather limited experimental evidence, suggested the linear relationship,

$$\frac{\sigma}{\sigma^*} = 1 + 0{\cdot}23\, M_E. \tag{6}$$

This empirical relation has been widely used in base-pressure analyses (e.g. References 3, 4 and 8).

Vasilu[28] based his estimate of σ (*see* Figure 10) upon slightly more extensive data. However, his variation of σ with Mach number was chosen to agree with the results of Anderson and Johns[22], whose data relate to fully developed, axisymmetric, turbulent jet mixing, and are not applicable to the free-jet boundary problem considered here, as Maydew and Reed[15] have pointed out.

McDonald[6], by considering a compressibility transformation, derived the equation,

$$\frac{\sigma}{\sigma^*} = 1 + \frac{\gamma - 1}{2} M_E{}^2. \tag{7}$$

This variation is plotted in Figure 10 for $\gamma = 1{\cdot}40$.

Channapragada[29, 30] has derived a semi-empirical relation between σ and Mach number, which predicts a strong influence of thermal level on the rate of spread of the mixing zone. For the particular case where total temperature is conserved across the shear layer, Channapragada's variation of σ/σ^* with Mach number is shown in Figure 10.

Since Channapragada's theoretical treatment is the most comprehensive available, and appears to agree with the limited experimental data fairly well, the variation of σ predicted by this method will be used in subsequent calculations.

2.5. *Effect of the Initial Boundary Layer.*

Kirk[5] proposed a simple method of allowing for the effect of initial boundary-layer thickness on the development of the shear layer. Nash[31] has shown that this method is in good agreement with more detailed and comprehensive calculations, made for the case of incompressible flow, and has pointed out that there is no obvious reason why the same should not be true for flow at higher Mach numbers.

In using Kirk's approximation, the real shear layer developing from an initial boundary layer is replaced by an equivalent 'asymptotic' shear layer growing from zero thickness over a greater distance (*see* Figure 11). The distance between the origin of the equivalent shear layer and the separation point (denoted x') can be simply related to the momentum thickness of the boundary layer immediately after the expansion. The results obtained for the asymptotic shear layer in Sections 2.2 and 2.4 may then be used for the equivalent shear layer.

The length of the origin shift (x') may be found by equating the momentum thickness of the boundary layer at the end of the expansion to the momentum thickness of a free-shear layer after it has grown over the distance x'.

The momentum thickness of a free-shear layer at any axial distance (x) is given by

$$\theta_s = \int_{-\infty}^{+\infty} \frac{\rho u}{\rho_E u_E}\left(1 - \frac{u}{u_E}\right) dy \tag{8}$$

Using equations (A7) and (A9) of Appendix II and the dimensionless co-ordinate

$$\eta = \frac{\sigma y}{x}$$

equation (8) becomes

$$\theta_s = \int_{-\infty}^{\infty} \frac{(1-C_E{}^2)\phi(1-\phi)}{(1-C_E{}^2\phi^2)} \frac{x}{\sigma}\, d\eta$$

or

$$\frac{\sigma\theta_s}{(1-C_E{}^2)x} = \int_{-\infty}^{\infty} \frac{\phi(1-\phi)}{(1-C_E{}^2\phi^2)}\, d\eta\,. \tag{9}$$

If $\theta_s = \theta_1$, the momentum thickness of the boundary layer after it has negotiated the expansion, then equation (9) gives

$$x' = \frac{\sigma\theta_1}{I} \tag{10}$$

where x' is the equivalent shift of origin
and

$$I = (1-C_E{}^2)\int_{-\infty}^{\infty} \frac{\phi(1-\phi)}{(1-C_E{}^2\phi^2)}\, d\eta\,. \tag{11}$$

I, as defined by equation (11), is a function of Mach number and the shape of the shear-layer velocity profile. Using Crane's incompressible velocity distribution as before, to relate ϕ and η, I may be evaluated as a function of free-stream Mach number. By combining equations (4) and (11), I may be expressed in a simpler form as,

$$I = (1 - C_E^2) \int_{-\infty}^{\eta_M} \frac{\phi \, d\eta}{1 - C_E^2 \phi^2} \tag{12}$$

The variation of I with Mach number as computed from equation (12), using Crane's profile, is given in Figure 12, and this variation will be used in future calculations.

When Kirk's approximation is applied, the separation streamline (defined as the streamline which originates at the corner) is not coincident with the median streamline of the equivalent free-shear layer. The mass flux beneath the median streamline of the equivalent shear layer at the corner, q_s, is given by

$$\frac{q_s}{\rho_{E,1} u_{E,1}} = \int_{-\infty}^{y_M} \frac{\rho_1 u_1}{\rho_{E,1} u_{E,1}} \, dy = \frac{x'}{\sigma} \int_{-\infty}^{\eta_M} \frac{(1 - C_E^2)\phi}{(1 - C_E^2 \phi^2)} \, d\eta$$

$$= I \frac{x'}{\sigma} = \theta_1 \qquad \text{from equation (10)}$$

therefore

$$q_s = \rho_{E,1} u_{E,1} \theta_1 . \tag{13}$$

This mass flow, q_s, is equivalent to a quantity of bleed flow injected into the base region. If 'ψ' denotes the usual stream function,

$$\psi = \int \rho u \, dy \tag{14}$$

then we may write

$$q_s = \psi_M - \psi_s = \rho_{E,1} u_{E,1} \theta_1 \tag{15}$$

where ψ_M refers to the median streamline, and ψ_s refers to the separation streamline.

2.6. *Effect of Bleed Flow.*

If q is the quantity of bleed flow which is allowed to enter the cavity from an external source, then clearly the reattachment streamline (ψ_R) is given by the relationship

$$\psi_s - \psi_R = q . \tag{16}$$

As mentioned in Section 2.5, the initial boundary layer effectively introduces a further quantity of bleed flow (q_s) into the cavity. The total effective bleed flow in the cavity (q_{EFF}) is then given by

$$q_{\text{EFF}} = q_s + q = \psi_M - \psi_R . \tag{17}$$

If q_{EFF} and $C_{E,1}$ are specified, the velocity on the reattachment streamline (ϕ_R) at the reattachment point (neglecting for the moment the effects of recompression and considering the growth of the shear layer to be at constant pressure right up to the reattachment point) may be found from the relation,

$$q_{\text{EFF}} = \int_{y_R}^{y_M} \rho u \, dy .$$

therefore

$$\frac{q_{\text{EFF}}}{\rho_{E,1} u_{E,1}} = \frac{x}{\sigma} \int_{\eta_R}^{\eta_M} \frac{(1 - C_{E,1}^2)\phi}{(1 - C_{E,1}^2 \phi^2)} \, dy \tag{18}$$

where x is the total mixing length from the origin of the equivalent free shear layer to the reattachment point. Equation (18) may be solved to give the reattachment velocity (ϕ_R), by numerically integrating the right-hand side of the expression (using Crane's incompressible velocity profile for the relation between ϕ and η), and combining the results obtained in the previous sections.

If x_1 is the length of the shear layer from the separation point to the reattachment point, and ν is the Prandtl-Meyer angle corresponding to the local Mach number of the external stream, then approximately

$$x_1 = \frac{h}{\sin(\nu_{E,1} - \nu_{E,0})}. \tag{19}$$

The above equation is valid for the case of zero external bleed flow. When bleed is introduced, the reattachment streamline is displaced from the separation streamline, as already mentioned. Equation (19) may be modified to account for this, and the resulting expression is,

$$x_1 = \frac{\sigma h}{\sigma \sin(\nu_{E,1} - \nu_{E,0}) + \cos(\nu_{E,1} - \nu_{E,0})(\eta_s - \eta_R)}. \tag{20}$$

Since this correction is small, for small bleed flows, equation (19) will be used for bleed-flow computations.

Providing $0{\cdot}3 < \phi < 0{\cdot}7$, the approximate relation

$$\frac{d\eta}{d\phi} = 8{\cdot}065\phi^2 - 9{\cdot}455\phi + 4{\cdot}54 \tag{21}$$

is valid for Crane's incompressible profile.

If q_{EFF} is not excessive, then for the right-hand expression in equation (18), the quantity $d\eta/d\phi$ may be considered as approximately constant over the range of integration, and equal to the value at the mean value of ϕ, i.e.

$$\frac{d\eta}{d\phi} = 8{\cdot}065\left(\frac{\phi_R + \phi_M}{2}\right)^2 - 9{\cdot}455\left(\frac{\phi_R + \phi_M}{2}\right) + 4{\cdot}54 = m \quad \text{(say)} \tag{22}$$

substituting from equation (22) into equation (18) gives

$$\frac{q_{\mathrm{EFF}}\sigma}{x\rho_{E,1}u_{E,1}} = (1 - C_{E,1}^2)m \int_{\phi_R}^{\phi_M} \frac{\phi d\phi}{(1 - C_{E,1}^2\phi^2)}.$$

Therefore

$$\frac{q_{\mathrm{EFF}}\sigma}{x\rho_{E,1}u_{E,1}} = \frac{(1 - C_{E,1}^2)m}{2C_{E,1}^2} \log_e\left[\frac{1 - C_{E,1}^2\phi_R^2}{1 - C_{E,1}^2\phi_M^2}\right]. \tag{23}$$

If we define

$$C_q = \frac{q}{\rho_{E,1}u_{E,1}h}. \tag{24}$$

then equations (23) and (24) give

$$\frac{(\theta_1 + C_q h)\sigma}{x} = \frac{(1 - C_{E,1}^2)m}{2C_{E,1}^2} \log_e\left[\frac{1 - C_{E,1}^2\phi_R^2}{1 - C_{E,1}^2\phi_M^2}\right] \tag{25}$$

where

$$x = x' + x_1.$$

Figures 6, 9, 10 and 12, together with equations (10), (20), (22), and (25), enable a relationship between q, p_1/p_0 and ϕ_R to be determined.

2.7. *Reattachment Criteria.*

It will be observed from equation (25) that to close the base-pressure solution, that is, to obtain a unique relation between q and p_1/p_0 in terms of known quantities, a further relation for ϕ_R must be provided.

It has already been mentioned in Section 1 that, when the effect of the approaching boundary layer is taken into account, the simple 'escape' criterion of Chapman and Korst proves to be inadequate, and that, in order to obtain agreement between theory and experiment, it is necessary to assume that the reattachment streamline stagnates to the local pressure at the reattachment point (p_R), rather than to the pressure downstream of the recompression zone (p_2).

If the reattachment streamline stagnates isentropically, then

$$\left(\frac{p_R}{p_1}\right)^{(\gamma-1)/\gamma} = \frac{1}{1 - C_{E,1}{}^2 \phi_R{}^2} \tag{26}$$

and the problem becomes one of relating the reattachment pressure to the pressures at the beginning and end of the pressure rise.

Nash[4] has proposed using the factor N, where

$$N = \frac{p_R - p_1}{p_2 - p_1} \tag{27}$$

and has found that this has a value around 0·35, instead of unity as the 'escape' criterion implies. Unpublished work by the same author, however, has shown that the use of this factor is not very satisfactory, since it depends both on Reynolds number and Mach number.

The problem has therefore remained of finding a relation for the reattachment pressure (p_R). In this respect, it is useful to consider the similarity between the behaviour of a redeveloping boundary layer, as in the present flow model downstream of the reattachment point, and a separating boundary layer, such as occurs for example in the flow over a forward-facing step. Since both these phenomena belong to the same family of shock-wave boundary-layer interaction problems, it is reasonable to suppose that the large body of experimental and theoretical work which is available on boundary-layer separation may find application to our present flow model.

Most attempts at employing this analogy have concentrated on relating the 'peak' pressure rise associated with separation of a boundary layer to the total pressure rise (p_1 to p_2) at reattachment (e.g. Reference 32). Cortwright[33] suggested that a 'peak pressure ratio', which is a function only of Mach number, be used for forward- and backward-facing steps, blunt trailing edges and annular bases. This ratio was plotted against Mach number, and the data for all these cases fell into a narrow region. This criterion, in combination with the oblique shock equation, gave him a solution to the base-pressure problem.

Although the use of this 'peak pressure ratio' analogy gives qualitative agreement, as indicated by the experimental data in Reference 34, there is a distinct lack of quantitative correlation[35]. Since the pressure rise beyond the separation point for a turbulent boundary layer depends on the method which is used to induce separation (e.g. Reference 34), and the overall pressure rise for a reattaching boundary layer in the present flow model depends on the initial boundary-layer thickness, as well as on Mach number, it is not surprising that the correlation is rather poor.

A more satisfactory analogy may be found between the local pressure rise at reattachment ($p_r - p_2$) in the base flow model, and the pressure rise to the separation point ($p_0 - p_s$) for shock-induced separation of a boundary layer on a flat plate. This latter pressure rise has been found

experimentally to be independent of the mode of inducing separation[34], and, as in the case of the redeveloping boundary layer in the base flow model, is governed only by the balance which must exist between the growth of the boundary layer and its equilibrium with the free stream. Criteria which have been developed for predicting the pressure rise to separation $(p_0 - p_s)$ may therefore be expected to provide a useful guide to the problem of relating p_R to p_2.

Of the various methods available (e.g. References 7, 36, 37, 38) for predicting the pressure rise to separation for a turbulent boundary layer on a flat plate, that of Reshotko and Tucker[7] appears to be the most useful analysis for the present purpose. By using a form of the moment of momentum equation, they were able to show that, if friction can be neglected, then across a discontinuity,

$$\frac{M_2}{M_1} = \frac{f(H_2^*)}{f(H_1^*)} \tag{28}$$

where M is the free-stream Mach number, the subscript 1 refers to conditions ahead of the discontinuity and the subscript 2 to conditions behind the discontinuity. H^* is the transformed shape parameter, which is related to the compressible shape parameter (H) by the relation (for $\gamma = 1{\cdot}40$),

$$H = H^*(1 + 0{\cdot}2M^2) + 0{\cdot}2M^2 \tag{29}$$

also,

$$f(H^*) = \frac{H^{*2}}{(H^{*2} - 1)^{1/2}(H^* + 1)} e^{1/(H^*+1)} \tag{30}$$

Reshotko and Tucker applied these relations to the problem of shock-induced separation of a turbulent boundary layer, and showed that conditions across the interaction could be correlated in terms of Mach number ratio. In addition, Mager[36, 39] has suggested that the Mach number ratio to the separation point is constant.

A similar criterion may be considered for the base flow model. If p_1 is assumed, then the free-stream Mach number in the base region $(M_{E,1})$ and the downstream static pressure and free-stream Mach number $(M_{E,2})$ may be found. If the shear layer, and the free stream outside it, compress isentropically up to the reattachment pressure (p_R), then the relation between p_R and the free-stream Mach number $(M_{E,R})$ at the reattachment point is

$$\frac{p_R}{p_1} = \left[\frac{1 + 0{\cdot}2M_{E,1}^2}{1 + 0{\cdot}2M_{E,R}^2}\right]^{\gamma/(\gamma-1)} \tag{31}$$

By specifying R, where

$$R = \frac{M_{E,2}}{M_{E,R}} \tag{32}$$

a relationship for p_R may be found. From the analogy with shock-induced separation, discussed above, R could be expected to be sensibly constant.

McDonald has attempted to refine the above approach by using a modified form of equation (28), and calculating values of H^*. He suggested that (in the present notation),

$$\left(\frac{M_{E,2}}{M_{E,R}}\right)^{-1} = \frac{f(H_2^*)}{f(H_R^*)} = R^{-1} \tag{33}$$

which is clearly an inverted form of equation (28). By assuming that the whole shear layer compresses isentropically up to the reattachment pressure, H_R may be computed as a function of ϕ_R and $M_{E,1}$ (*see* Appendix IV, where the analysis is given), and hence, from equation (29), H_R^* may be found

as a function of ϕ_R and $M_{E,1}$. In Figure 14 the results of some calculations by the present author are plotted, based on the theory in Appendix IV, and using Crane's incompressible velocity profile for the shear layer. From this graph, $H_R{}^*$ may be estimated by interpolation, for any value of ϕ_M and $M_{E,1}$ and by using equation (30), or more conveniently Figure 15 (where this function is plotted), $f(H_R{}^*)$ may be found.

Clearly, if $H_2{}^*$ is specified, then equation (33) enables R to be found, and hence p_R, in the manner already described. McDonald has suggested that $H_2{}^* = 1{\cdot}40$ should be used as a reattachment criterion. This is an alternative to the Mach number ratio (R) criterion, and depends upon the introduction of two further assumptions into the base flow analysis:

(i) that the velocity profile at reattachment can be adequately estimated by assuming the shear layer to compress isentropically,

(ii) that the Reshotko and Tucker relation {equation (28)} may be used in an inverted form {equation (33)} for reattaching boundary layers.

Only an analysis of experimental data can decide whether this refinement produces any significant improvement over the Mach number ratio criterion.

3. *Comparison with Experiment.*

If the base pressure for a particular set of conditions is known from experiment, then the foregoing treatment may be used to evaluate the quantities N, R and $H_2{}^*$. By analysing the available data in this way, comparisons may be made between these different forms of reattachment criterion and their relative usefulness judged.

The answers obtained will depend on whether the recompression of the free stream is assumed to be isentropic, or to obey oblique shock-wave relationships. In what follows, the results of using both these assumptions will be compared. The specific heat ratio (γ) is taken to be $1{\cdot}40$ throughout.

3.1. *Zero Bleed Flow.*

Experimental results from References 8, 40, 41, 42, 43 and 47 have been analysed. In References 8, 40, 41 and 47 the base pressure was measured for backward-facing steps, and the initial boundary-layer momentum thickness, Mach number and flow geometry are specified. In References 42 and 43, the base pressure on blunt trailing-edge aerofoil sections was measured and a range of chord Reynolds number. In these latter cases, the minimum base pressure recorded has been taken, since this corresponds to transition from laminar to turbulent flow at the expansion corner (*see* References 1 and 40), and the initial turbulent boundary layer then has its minimum thickness. The initial boundary-layer momentum thickness may be readily estimated from the chord Reynolds number, since the boundary layer will be laminar up to the trailing edge at this minimum base-pressure condition. In Table 2 a key is given to the symbols used for these data in Figures 16 to 22.

Chapman *et al*[45] have also measured the base pressure for blunt trailing-edge wings in supersonic turbulent flow, where the transition point was well forward of the trailing edge. The initial momentum thickness for their tests, however, covers a greater range than can properly be treated by the present method, which is valid for thin boundary layers only. A comparison between the theory and Chapman's results will be given later.

The data of Fuller and Reid[46] are not in line with those of other workers at neighbouring Mach numbers, as Nash[4] has pointed out, and their results will not be used in this analysis.

In Figures 16, 17, 18 and 19, the computed values of N, R, $H_R{}^*$, $f(H_R{}^*)$ and $H_2{}^*$ are plotted against the Mach number in the base region ($M_{E,1}$) for both isentropic and oblique shock-wave recompression.

In Figure 16, N is seen to vary between $0{\cdot}1$ and $0{\cdot}5$, and the scatter of the points is considerable for both forms of recompression. It would therefore appear that Nash's reattachment criterion of $N = 0{\cdot}35$ provides a rather poor correlation of the data.

A much improved correlation is shown in Figure 17, where R is plotted against $M_{E,1}$, the scatter of the points being least for the case of oblique shock-wave recompression. Here the empirical relation

$$R = 0{\cdot}799 + 0{\cdot}1560M_{E,1} - 0{\cdot}08237M_{E,1}{}^2 + 0{\cdot}009564M_{E,1}{}^3 \tag{34}$$

gives a good fit to the data.

Figure 18 illustrates the variation of $H_R{}^*$ and $f(H_R{}^*)$ with $M_{E,1}$, computed by the method indicated in Section 2.7. Although the value of $H_R{}^*$ varies between $2{\cdot}0$ and $2{\cdot}5$, with fairly pronounced scatter, the quantity $f(H_R{}^*)$ is little affected by these variations and has an approximately constant value of $1{\cdot}05$.

Using the results given in Figure 18, $H_2{}^*$ was computed by the method discussed in Section 2.7, and the results are given in Figure 19. The data indicate that $H_2{}^*$ does not have a constant value of $1{\cdot}40$, as McDonald suggests, but varies with $M_{E,1}$. Since $f(H_R{}^*)$ is almost constant, it is apparent from equation (33) that a correlation in terms of $H_2{}^*$ is effectively equivalent to one in terms of R. Comparison of Figures 17 and 19 shows that in fact no significant reduction in the scatter of the data is achieved by introducing McDonald's refinement.

From the available data it is therefore concluded that the most convenient correlation is of the form given in Figure 17, with oblique shock-wave recompression.

The analogy with separation, discussed in Section 2.7, suggests that the value of R should be constant, and it is at first sight surprising that the analysis of experimental data shows it to depend significantly on $M_{E,1}$. It is worth remembering, however, that the assumed properties of the shear layer are uncertain at high values of $M_{E,1}$. For example, the velocity profile used in the calculation has only been verified by Maydew and Reed[15] for Mach numbers up to 2. As all the computed points in Figures 16 to 19 relate to $M_{E,1} > 2$, it is probable that this apparent variation of reattachment parameters with $M_{E,1}$ is a reflection of an incorrect extrapolation of shear-layer properties. Were knowledge of these available at higher speeds, it could well be that a constant value for R would appear.

However, for the present, we are compelled to accept the empirical relation given by equation (34). Some compensation for the probable errors in this equation, as described above, is inherent in its use to predict base pressure under the conditions for which it was derived, that is to say for zero bleed flow.

3.2. *Bleed Flow.*

Carrière and Sirieix[8] have investigated the effect of introducing bleed air into the base region of a backward-facing step in supersonic two-dimensional turbulent flow. In these experiments, $M_{E,1}$ was kept constant for a range of bleed mass-flow addition by suitably varying the angle of a wedge in the reattachment region. Variation of the quantity R computed from these results is plotted against the bleed mass-flow coefficient (C_q) in Figure 20, for values of $M_{E,1}$ between $2{\cdot}15$ and $3{\cdot}70$.

At the lowest Mach number, R is almost independent of C_q, whilst at higher Mach numbers it becomes significantly dependent on C_q, R tending to increase as C_q increases. Although further data will be required before any positive conclusion can be stated as to the effect of C_q on R, it would appear that the reattachment criterion proposed in Section 3.1 {equation (34)}, when used for predicting bleed-flow effects, is valid only for the range $M_{E,1} < 2{\cdot}5$. This limitation may be due to incorrect assumptions concerning the velocity profile in the shear layer at high Mach numbers, as discussed in the previous section.

4. *Prediction of Base Pressure.*

The foregoing analysis enables a method of predicting base pressures to be formulated.

From equations (25), (26) and (31),

$$\frac{(\theta_1 + C_q h)\sigma}{x} = \frac{(1 - C_{E,1}{}^2)m}{2C_{E,1}{}^2} \log_e \left[\frac{1 + 0{\cdot}2\left(\frac{M_{E,2}}{R}\right)^2}{(1 + 0{\cdot}2M_{E,1}{}^2)(1 - C_{E,1}{}^2 \phi_M{}^2)} \right] \tag{35}$$

where:

(i) $\frac{\theta_1}{\theta_0}$ is determined from Figure 6.

(ii) C_q is determined from equation (24).

(iii) σ is determined from Channapragada's variation of σ with Mach number ($M_{E,1}$) given in Figure 10.

(iv) $x = x' + x_1$

where

$x' = \sigma\theta_1/I$,

I being determined from Figure 12

and

$$x_1 = \frac{h}{\sin(\nu_{E,1} - \nu_{E,0})}.$$

(v) m is determined from equation (22).

(vi) $M_{E,2}$ is determined from the oblique shock relationship.

(vii) R is determined from equation (34).

(viii) ϕ_M is determined from equation (5).

(ix) $M_{E,1}$ and $C_{E,1}$ are determined from p_1/p_0 and M_0.

Thus if $M_{E,0}$, θ_0/h, q and the model geometry are specified, equation (35) may be solved iteratively for $M_{E,1}$ and hence p_1/p_0.

In Figures 21 and 22, the variation of p_1/p_0 with θ_0/h as computed by the present method, for $M_{E.0}$ of 2·0 and 3·0 respectively, and zero bleed flow, is compared with the corresponding variations predicted by the methods of Nash and McDonald and the available experimental data at these Mach numbers. The present theory is in good agreement with the data (Table 2) for small values of θ_0/h. At the higher values of θ_0/h, reasonably close agreement with the results of Chapman *et al* can be obtained at an $M_{E,0}$ of 3·0. Overall, the agreement is felt to be an improvement on that obtained by previous methods, particularly for thin boundary layers.

5. *Conclusions.*

The prediction of base pressure in two-dimensional supersonic turbulent flow is considered in detail, and various modifications to the theoretical analysis of the flow model are suggested. Several reattachment criteria are examined and compared in the light of experimental data, and preference is accorded to a simple criterion in terms of a Mach number ratio. This relates the Mach numbers corresponding to the reattachment and final pressures, and an empirical relationship for this ratio is given which may be easily incorporated into the base flow analysis.

The success of this Mach number ratio as a criterion for reattachment is reminiscent of shock-induced separation in supersonic flow, and suggests some quite close analogy between the two forms of shock boundary-layer interaction.

REFERENCES

No.	*Author(s)*	*Title, etc.*
1	L. Crocco and L. Lees ..	A mixing theory for the interaction between dissipative flows and nearly isentropic streams. *J. Ae. Sci.*, Vol. 19, p. 649. October, 1952.
2	D. R. Chapman	An analysis of base pressure at supersonic velocities and comparison with experiment. N.A.S.A. Tech. Note 2137. July, 1950.
3	H. H. Korst	A theory for base pressures in transonic and supersonic flow. *J. App. Mech.*, Vol. 23, No. 4, p. 593. December, 1956.
4	J. F. Nash	An analysis of two-dimensional turbulent base flow, including the effect of the approaching boundary layer. A.R.C. R. & M. 3344. July, 1962.
5	F. N. Kirk	An approximate theory of base pressure in two-dimensional flow at supersonic speeds. R.A.E. Tech. Note Aero. 2377. March, 1954. (Issued December, 1959).
6	H. McDonald	Turbulent shear layer reattachment with special emphasis on the base pressure problem. B.A.C. Report Ae 175, Issue 2. August, 1963.

REFERENCES—*continued*

No.	*Author(s)*	*Title, etc.*
7	E. Reshotko and M. Tucker ..	Effect of a discontinuity on turbulent boundary-layer-thickness parameters with application to shock-induced separation. N.A.C.A. Tech. Note 3454. May, 1955.
8	P. Carriére and M. Sirieix ..	Facteurs d'influence du recollement d'un ecoulement supersonique. Paper presented at the 10th International Congress of Applied Mechanics, Stresa. O.N.E.R.A. Memo. Tech. 20. 1961.
9	W. Tollmien	Berechnung der turbulenten Ausbreitungsvorgaenge. *Z.A.M.M.*, Vol. 6, pp. 468 to 478. 1926. (Also N.A.C.A. Tech. Memo. 1085. 1945).
10	H. Görtler	Berechnung von Aufgaben der freien Turbulenz auf Grund eines neuen Näherungsansatzes. *Z.A.M.M.*, Vol. 22, p. 244, 1942 (translated as R.T.P. Trans. 2234. 1944) A.R.C. 7947.
11	G. N. Abramovitch	The theory of a free-jet of a compressible gas. Central Aero. Hydrodynamical Institute, Moscow, Report 377. 1939. (Translated as N.A.C.A. Tech. Memo. 1058. 1944.)
12	L. J. Crane	The laminar and turbulent mixing of jets of compressible fluids. *J. Fluid Mech.*, Vol. 3, Part I. October, 1957.
13	L. Prandtl	Bericht über Untersuchungen zer ausgebildeten Turbulenz. *Z.A.M.M.*, Vol. 5, p. 136. 1925.
14	L. Prandtl	Bemerkungen zur Theorie der freien Turbulenz. *Z.A.M.M.*, Vol. 22, p. 241. 1942.
15	R. C. Maydew and J. F. Reed ..	Turbulent mixing of axisymmetric compressible jets (in the half-jet region) with quiescent air. Sandia Corporation Research Report SC4764 (RR) also A.R.C. 24 941. March, 1963.
16	H. Reichardt	Gesetzmässigkeiten der freien Turbulenz. V.D.I.—*Forschugnsheft*, No. 414, 1942. (Translated as R.T.P. Trans. 1752, A.R.C. 6670.)
17	H. W. Liepmann and J. Laufer	Investigation of free turbulent mixing. N.A.C.A. Tech. Note 1257. August, 1947.
18	P. B. Gooderum, G. P. Wood and M. J. Brevoort.	Investigation with an interferometer of the turbulent mixing of a free supersonic jet. N.A.C.A. Report 963. 1950.
19	D. Bershader and S. I. Pai ..	On turbulent mixing in two-dimensional supersonic flow. *J. App. Phys.*, Vol. 21, No. 6. 1950.

REFERENCES—*continued*

No.	*Author(s)*	*Title, etc.*
20	B. B. Carey	An optical study of two-dimensional jet mixing. Ph.D. Thesis, Department of Physics, University of Maryland. 1954.
21	S. I. Pai	*Fluid Dynamics of Jets.* Chapter 5, p. 101. D. Van Nostrand Co., Inc., New York. 1954.
22	A. R. Anderson and F. R. Johns	Characteristics of free supersonic jets, exhausting into quiescent air. *Jet Propulsion*, Vol. 25, No. 1. 1955.
23	N. H. Johannesen	The mixing of free axially-symmetrical jets of Mach number 1·40. A.R.C. R. & M. 3291. January, 1957.
24	N. H. Johannesen	Further results on the mixing of free axially symmetric jets of Mach number 1·40. A.R.C. R. & M. 3292. May, 1959.
25	A. F. Charwat and J. K. Yakura	An investigation of two-dimensional supersonic base pressure. *J. Ae. Sci.*, Vol. 25, p. 122. February, 1958.
26	E. T. Pitkin and I. Glassman ..	Experimental mixing profiles of a Mach 2·6 free jet. *J. Ae. Sci.*, Vol. 25, p. 791. December, 1958.
27	H. H. Korst and W. Tripp ..	The pressure on a blunt trailing edge separating two supersonic two-dimensional air streams of different Mach numbers and stagnation pressures, but identical stagnation temperatures. Paper presented at the Mid-West Conference on solid and fluid mechanics, University of Michigan. April, 1957.
28	J. Vasilu	Pressure distribution in regions of step-induced turbulent separation. *J. Ae Sci.*, Vol. 29, No. 5. May, 1962.
29	R. S. Channapragada	A compressible jet spread parameter for mixing zone analyses. Part I. United Technology Center. Tech. Memo. 14–63–U25. May, 1963.
30	R. S. Channapragada	A compressible jet spread parameter for mixing zone analyses. Part II. United Technology Center, Tech. Memo. 14–63–U31. June, 1963.
31	J. F. Nash	The effect of an initial boundary layer on the development of a turbulent free shear layer. A.R.C. C.P. 682. June, 1962.
32	E. S. Love	Base pressure at supersonic speeds on two-dimensional airfoils and on bodies of revolution with and without fins having turbulent boundary layers. N.A.C.A. Tech. Note 3819. January, 1957.
33	E. M. Cortwright, Jr.	Some aerodynamic considerations of nozzle-afterbody combinations. *Aero. Eng. Rev.*, Vol. 15, No. 9, pp. 59 to 65. September, 1956.

REFERENCES—*continued*

No.	*Author(s)*	*Title, etc.*
34	D. R. Chapman, D. M. Kuehn and H. K. Larson.	Investigation of separated flows in supersonic streams and subsonic streams with emphasis on the effect of transition. N.A.C.A. Report 1356. 1958.
35	L. E. Baughman and F. D. Kochendorfer.	Jets effects on base pressures of conical afterbodies at Mach 1·91 and 3·12. N.A.C.A. Research Memo. E57E06. August, 1957.
36	A. Mager	Prediction of shock-induced turbulent boundary layer separation. *J. Ae. Sci.*, Vol. 22, No. 3, pp. 201 to 202. March, 1955.
37	R. D. Tyler and A. H. Shapiro	Pressure rise required for separation in interaction between turbulent boundary layer and shock wave. *J. Ae. Sci.*, Vol. 20, No. 12, pp. 858 to 860. December, 1953.
38	L. Crocco and R. F. Probstein	The peak pressure rise across an oblique shock emerging from a turbulent boundary layer over a plane surface. Report 254, Dept. Aero. Eng., Princeton University. March, 1954.
39	A. Mager	On the model of the free shock-separated, turbulent boundary layer. *J. Ae. Sci.*, Vol. 23, No. 2, p. 181. February, 1956.
40	M. Sirieix	Pression du culot et processus de melange turbulent en ecoulement supersonique plan. *La Recherche Aeronautique*, No. 78, p. 13. September/October, 1960.
41	H. Thomann	Measurements of heat transfer and recovery temperature in regions of separated flow at a Mach number of 1·8. F.F.A. Report 82. Sweden. 1959.
42	G. E. Gadd, D. W. Holder and J. D. Regan.	Base pressure in supersonic flow. A.R.C. C.P. 271. March, 1955.
43	V. Van Hise	Investigation of variation in base pressure over the Reynolds number range in which wake transition occurs for two-dimensional bodies at Mach numbers from 1·95 to 2·92. N.A.S.A. Tech. Note D–167. November, 1959.
44	M. A. Badrinarayanan	An experimental investigation of base flows at supersonic speeds. *J.R.Ae.S.*, Vol. 65, p. 475. July, 1961.
45	D. R. Chapman, W. R. Wimbrow and R. H. Kester.	Experimental investigation of base pressure on blunt trailing-edge wings at supersonic velocities. N.A.C.A. Report 1109. 1952.
46	L. Fuller and J. Reid	Experiments on two-dimensional base flow at $M = 2·4$. A.R.C. R. & M. 3064. February, 1956.
47	R. C. Hastings	Turbulent flow past two-dimensional bases in supersonic streams. A.R.C. R. & M. 3401. December, 1963.

TABLE 1

A Comparison of Velocity Profiles

η	ϕ			
	Görtler[10]	Crane[12]	Error function $\phi = \frac{1}{2}(1+\text{erf}\,\eta)$	Tollmien[9]
$-\infty$	0	0	0	0
−2·6	0·003	—	—	—
−2·4	0·006	—	—	—
−2·2	0·010	—	0·001	—
−2·0	0·017	0·023	0·002	—
−1·8	0·026	0·032	0·005	—
−1·6	0·039	0·045	0·012	0·003
−1·4	0·056	0·064	0·021	0·017
−1·2	0·079	0·089	0·045	0·044
−1·0	0·111	0·123	0·079	0·092
−0·8	0·155	0·169	0·129	0·151
−0·6	0·214	0·228	0·198	0·220
−0·4	0·292	0·304	0·286	0·306
−0·2	0·388	0·395	0·389	0·400
0	0·500	0·500	0·500	0·500
+0·2	0·619	0·612	0·611	0·605
+0·4	0·733	0·722	0·714	0·707
+0·6	0·832	0·819	0·802	0·802
+0·8	0·905	0·894	0·871	0·887
+1·0	0·953	0·945	0·921	0·949
+1·2	0·980	0·975	0·955	0·983
+1·4	0·993	0·990	0·976	—
+1·6	0·998	0·997	0·988	—
+1·8	—	0·999	0·995	—
+2·0	—	—	0·998	—
$+\infty$	1·0	1·0	1·0	1·0

TABLE 2

Symbols Used for Experimental Results

Author	Reference No.	Symbol	$M_{E,o}$	$\frac{\theta_o}{h}$	$M_{E,1}$
Carriere and Sirieix	8	■	2·000	0·0145	2·150
		■	2·000	0·0145	2·350
		■	2·000	0·0145	2·650
		■	3·000	0·0185	3·000
		■	3·000	0·0185	3·350
		■	3·000	0·0185	3·700
Sirieix	40	●	2·025	0·0300	2·654
		●	2·025	0·0200	2·695
		●	2·025	0·0150	2·718
		●	2·025	0·0120	2·747
Hastings	47	▼	1·560	0·0225	2·058
		▼	2·410	0·0221	3·314
		▼	3·100	0·0248	4·362
Thomann	41	▲	1·800	0·0461	2·332
G. E. Gadd et al.	42	○	1·500	0·0170	2·056
		○	2·000	0·0120	2·732
		○	3·000	0·0050	4·317
		○	3·000	0·0040	4·422
V. Van Hise	43	△	1·950	0·0075	2·702
		△	2·220	0·0060	3·180
		△	2·920	0·0050	4·223
M. A. Badrinarayanan	44	□	2·07	0·0500	2·596

N.B. Filled symbols denote tests on backward-facing steps. Unfilled symbols denote tests on aerofoil and blunt trailing-edge sections.

APPENDIX I

Symbols and Definitions

A	Defined by equation (A31)
C	Crocco number
C_p	Specific heat at constant pressure
C_q	Bleed flow coefficient {defined by equation (24)}
F	A non-dimensional stream function {defined by equation (A17)}
$f(H^*)$	A function of H^* {defined by equation (30)}
H	Shape parameter $= \frac{\delta^*}{\theta}$
h	Step height (*see* Figure 1)
I	A function of Mach number {defined by equation (12)}
I_1	Defined by equation (A32)
I_2	Defined by equation (A39)
I_3	Defined by equation (A45)
K	$\left(\frac{p_1}{p_0}\right)^{(\gamma-1)/\gamma}$
l	$\left(\frac{p_R}{p_1}\right)^{(\gamma-1)/\gamma}$
M	Mach number
m	$= \frac{d\eta}{d\phi}$, defined by equation (22)
N	A reattachment parameter, defined by equation (27)
n	Power law exponent of boundary-layer velocity profile
p	Static pressure
q	Bleed mass flow per unit width
q_s	$= \rho_{E,1}\, u_{E,1}\, \theta_1$
q_{EFF}	$= q + q_s$
R	A reattachment parameter, defined by equation (32)
r	A function of Mach number, defined by equation (A18)

T	Static temperature
u	Velocity
x, y	Co-ordinates of the shear layer
x'	Equivalent shift of the shear-layer origin
x_1	Distance from separation point to reattachment point
γ	Specific heat ratio
δ	Boundary-layer thickness
δ^*	Boundary-layer displacement thickness
η	Dimensionless co-ordinate of the shear layer $= \frac{\sigma y}{x}$
θ_0	Momentum thickness of boundary layer before expansion
θ_1	Momentum thickness of boundary layer after expansion
θ_s	Momentum thickness of shear layer
ν	Prandtl-Meyer angle
ρ	Density
σ	Jet spreading parameter
ϕ	Velocity ratio $= \frac{u}{u_E}$
ψ	Stream function $= \int \rho u \, dy$

Suffices

0	Initial conditions far upstream
1	Conditions in the shear-layer region
2	Conditions downstream of the recompression region
$*$	Incompressible equivalent (except for δ^*)
E	Conditions outside the viscous layer
M	Median streamline conditions
R	Reattachment conditions
s	Separation streamline conditions
t	Stagnation

If the initial boundary-layer profile is represented by the usual power law; i.e.

$$\frac{y_0}{\delta_0} = \phi_0{}^n \tag{A11}$$

then equation (A10) may be rewritten as,

$$\frac{\rho_{E,1}u_{E,1}}{\rho_{E,0}u_{E,0}(1-C_{E,0}{}^2)n}\frac{\theta_1}{\delta_0} = \int_0^1 \frac{\phi_0{}^2 d\phi_0}{(1-C_{E,0}{}^2\phi_0{}^2)} - \int_0^1 \frac{\phi_0{}^n[KC_{E,0}{}^2\phi_0{}^2-(K-1)]^{1/2}}{(1-C_{E,0}{}^2\phi_0{}^2)C_{E,0}}d\phi_0. \tag{A12}$$

If $K = 1$, $\theta_1 = \theta_0$, and equation (A12) reduces to,

$$\frac{\theta_0}{(1-C_{E,0}{}^2)n\delta_0} = \int_0^1 \frac{\phi_0{}^n(1-\phi_0)d\phi_0}{(1-C_{E,0}{}^2\phi_0{}^2)}. \tag{A13}$$

Dividing equation (A12) by (A13) gives,

$$\frac{\rho_{E,1}u_{E,1}\theta_1}{\rho_{E,0}u_{E,0}\theta_0} = \frac{\displaystyle\int_0^1 \frac{\phi_0{}^n d\phi_0}{1-C_{E,0}{}^2\phi_0{}^2} - \int_0^1 \frac{\phi_0{}^n[KC_{E,0}{}^2\phi_0{}^2-(K-1)]^{1/2}d\phi_0}{(1-C_{E,0}{}^2\phi_0{}^2)C_{E,0}}}{\displaystyle\int_0^1 \frac{\phi_0{}^n(1-\phi_0)d\phi_0}{(1-C_{E,0}{}^2\phi_0{}^2)}}. \tag{A14}$$

Also, from one-dimensional isentropic relations,

$$\frac{\rho_{E,1}u_{E,1}}{\rho_{E,0}u_{E,0}} = \frac{M_{E,1}(1+0\cdot2M_{E,0}{}^2)^3}{M_{E,0}(1+0\cdot2M_{E,1}{}^2)^3}. \tag{A15}$$

Equations (A14) and (A15) enable θ_1/θ_0 to be determined for particular values of p_1/p_0, $M_{E,0}$ and n.

APPENDIX III

Abramovitch's Method of Determining the Variation of Median Velocity Ratio with Mach Number

Abramovitch has considered the problem of compressible jet mixing up to the speed of sound. This theory was based on Taylor's concept of 'transport of vorticity', and leads to the differential equation,

$$F''' = -F\sqrt{(1+rF'^2)} + \frac{rF'F''^2}{1+rF'^2} \tag{A16}$$

where

$$F = \int \frac{\rho u}{\rho_E u_E}\, d\eta \tag{A17}$$

and the symbol $'$ refers to differentiation with respect to the non-dimensional co-ordinate (η). Also

$$r = 2(\gamma-1)M_E^2\left[1+\frac{\gamma-1}{2}M_E^2\right] \tag{A18}$$

The boundary conditions are

$$F(\eta_1) = \eta_1, \qquad F'(\eta_1) = 1, \qquad F''(\eta_1) = 0$$
$$F'(\eta_2) = 0, \qquad F''(\eta_2) = 0.$$

where η_1, η_2 are the co-ordinate limits of the shear layer.

At low speeds, when M_E is effectively zero, equation (A18) reduces to

$$F''' = -F \tag{A19}$$

which is the equation obtained by Tollmien from mixing-length considerations. Abramovitch's method may therefore be regarded as an extrapolation of Tollmien's solution.

To solve equation (A16), a numerical integration technique must be used. Abramovitch used a method based on the Taylor series to integrate the equation (which must be solved by a trial and error method, to satisfy the boundary conditions) for values of Mach number (M_E) ranging from zero to unity. These calculations have been extended by the present author to include Mach numbers up to 3·0. Once a velocity profile has been generated by integrating equation (A16) for a particular value of M_E, such that the boundary conditions are fulfilled, the median velocity may readily be found from the condition that,

$$F(\eta_M) = 0. \tag{A20}$$

From equation (A24), when

$$C_1 = \phi_R C_{E,1}$$

$$l = \frac{1}{1 - \phi_R{}^2 C_{E,1}{}^2}. \tag{A29}$$

Using equation (A29), equation (A28) may be simplified to give,

$$\delta_R = \left(\frac{p_R}{p_1}\right)^{-1/\gamma} \frac{x}{\sigma} \frac{1}{l^{1/2}} \int_{\eta_R}^{\eta_{\phi=1}} \frac{d\eta}{\left[1 - \left(\frac{\phi_R}{\phi}\right)^2\right]^{1/2}}. \tag{A30}$$

Putting

$$A = \left(\frac{p_R}{p_1}\right)^{-1/\gamma} \frac{x}{\sigma} \tag{A31}$$

and

$$I_1 = \frac{1}{l^{1/2}} \int_{\eta_R}^{\eta_{\phi=1}} \frac{d\eta}{\left[1 - \left(\frac{\phi_R}{\phi}\right)^2\right]^{1/2}} \tag{A32}$$

equations (A30), (A31) and (A32) yield,

$$\underline{\delta_R = AI_1}. \tag{A33}$$

The displacement thickness is defined by,

$$\delta^* = \int_0^{\delta} \left(1 - \frac{\rho u}{\rho_E u_E}\right) dy \tag{A34}$$

therefore

$$\delta_R{}^* = \delta_R - \frac{\rho_{E,1} u_{E,1}}{\rho_{E,R} u_{E,R}} \int_0^{\delta_R} \frac{\rho_R u_R}{\rho_{E,1} u_{E,1}} dy_R. \tag{A35}$$

Combining equations (A21) and (A35) gives,

$$\delta_R{}^* = \delta_R - \frac{\rho_{E,1} u_{E,1}}{\rho_{E,R} u_{E,R}} \int_{y_{R,1}}^{y_{E,1}} \frac{\rho_1 u_1}{\rho_{E,1} u_{E,1}} dy_1. \tag{A36}$$

If the total temperature across the boundary layer is conserved, we have (*see* Appendix II),

$$\frac{\rho}{\rho_E} = \frac{1 - C_E{}^2}{1 - C_E{}^2 \phi^2}. \tag{A37}$$

Combining equation (A36) with equations (A23), (A26) and (A37) gives,

$$\delta_R{}^* = \delta_R - \left(\frac{p_R}{p_1}\right)^{1/\gamma} \frac{x}{\sigma} \frac{C_{E,1}}{C_{E,R}} (1 - C_{E,1}{}^2) \int_{\eta_R}^{\eta_{\phi=1}} \frac{\phi d\eta}{(1 - C_{E,1}{}^2 \phi^2)}. \tag{A38}$$

If

$$I_2 = \int_{\eta_R}^{\eta_{\phi=1}} \frac{\phi d\eta}{(1 - C_{E,1}{}^2 \phi^2)} \tag{A39}$$

then equations (A31), (A38) and (A39) produce

$$\underline{\delta_R{}^* = \delta_R - \frac{AC_{E,1}(1 - C_{E,1}{}^2)}{C_{E,R}} I_2}. \tag{A40}$$

The momentum thickness is defined by,

$$\theta = \int_0^{\delta} \frac{\rho u}{\rho_E u_E}\left(1 - \frac{u}{u_E}\right) dy. \tag{A41}$$

Combining equations (A34) and (A41) gives,

$$\theta_R = \delta_R - \delta_R{}^* - \int_0^{\delta_R} \frac{\rho_R u_R{}^2}{\rho_{E,R} u_{E,R}{}^2}\, dy_R \tag{A42}$$

which may be rewritten as, {using equation (A21)},

$$\theta_R = \delta_R - \delta_R{}^* - \frac{\rho_{E,1}{}^2 u_{E,1}{}^2}{\rho_{E,R}{}^2 u_{E,R}{}^2} \int_{y_{R,1}}^{y_{E,1}} \frac{\rho_1 u_1{}^2}{\rho_{E,1}{}^2 u_{E,1}{}^2} \frac{u_R}{u_1}\, dy_1. \tag{A43}$$

Equations (A23), (A25), (A26) and (A37), in conjunction with equation (A43), yield,

$$\theta_R = \delta_R - \delta_R{}^* - \left(\frac{p_R}{p_1}\right)^{-1/\gamma} \frac{x}{\sigma} \frac{C_{E,1}{}^2}{C_{E,R}{}^2} (1 - C_{E,1}{}^2) \int_{\eta_R}^{\eta_\phi = 1} \frac{[lC_{E,1}{}^2 - (l-1)]^{1/2}\phi}{(1 - C_{E,1}{}^2\phi^2) C_{E,1}}\, d\eta \tag{A44}$$

If

$$I_3 = \int_{\eta_R}^{\eta_\phi = 1} \frac{[lC_{E,1}{}^2\phi^2 - (l-1)]^{1/2}\, \phi\, d\eta}{(1 - C_{E,1}{}^2\phi^2)}. \tag{A45}$$

Then equations (A31), (A44) and (A45) produce,

$$\underline{\theta_R = \delta_R - \delta_R{}^* - \frac{A C_{E,1}(1 - C_{E,1}{}^2)}{C_{E,R}{}^2} I_3} \tag{A46}$$

The shape parameter (H) is defined by,

$$H = \frac{\delta^*}{\theta}. \tag{A47}$$

From equations (A33), (A40) and (A46),

$$\underline{\underline{H_R = \frac{\left(\frac{C_{E,R}{}^2}{1 - C_{E,1}{}^2}\right) I_1 - C_{E,R}\, C_{E,1} I_2}{C_{E,R}\, C_{E,1} I_2 - C_{E,1} I_3}}}. \tag{A48}$$

Since I_1, I_2 and I_3 are functions of p_R/p_1 and $M_{E,1}$, H_R is also a function of p_R/p_1 and $M_{E,1}$. Since specifying ϕ_R and $M_{E,1}$ also specifies p_R/p_1 we have

$$\underline{H_R = f(\phi_R, M_{E,1})}. \tag{A49}$$

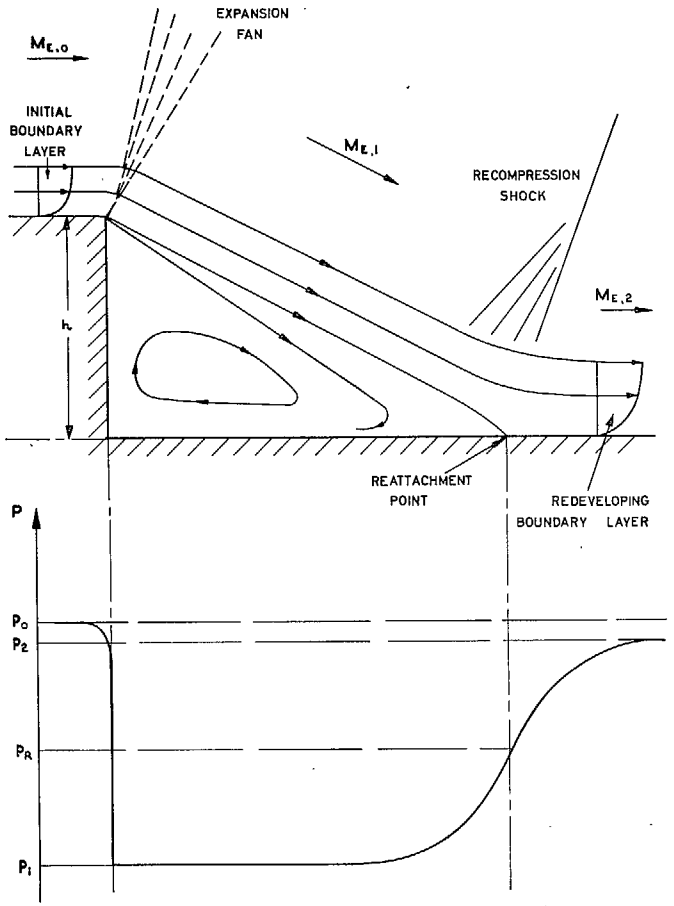

FIG. 1. Supersonic flow over a backward-facing step.

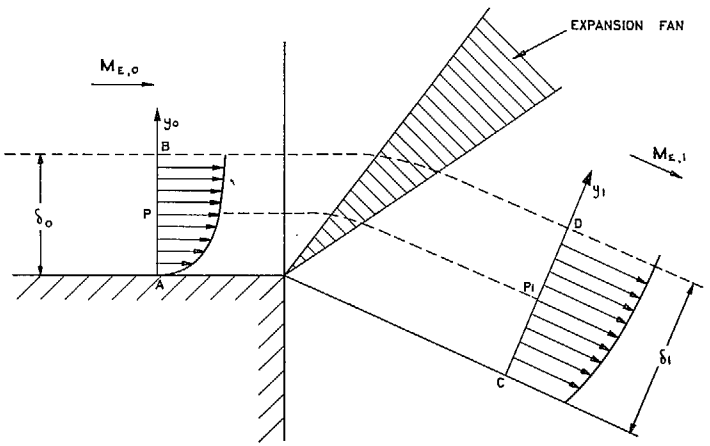

FIG. 2. Flow model at the expansion corner.

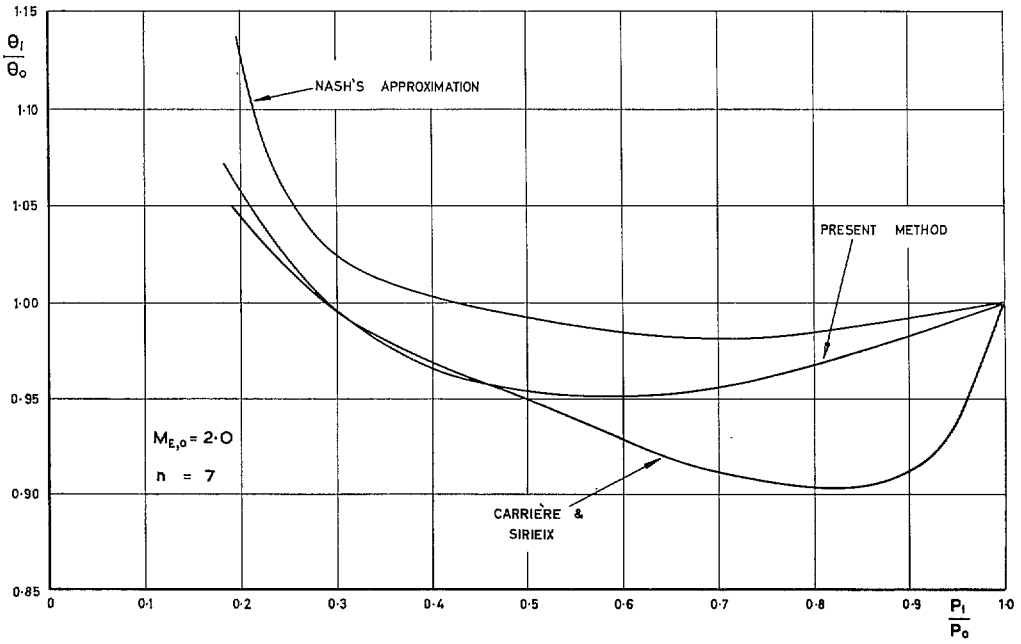

FIG. 3. Effect of abrupt expansion on boundary-layer momentum thickness—I.

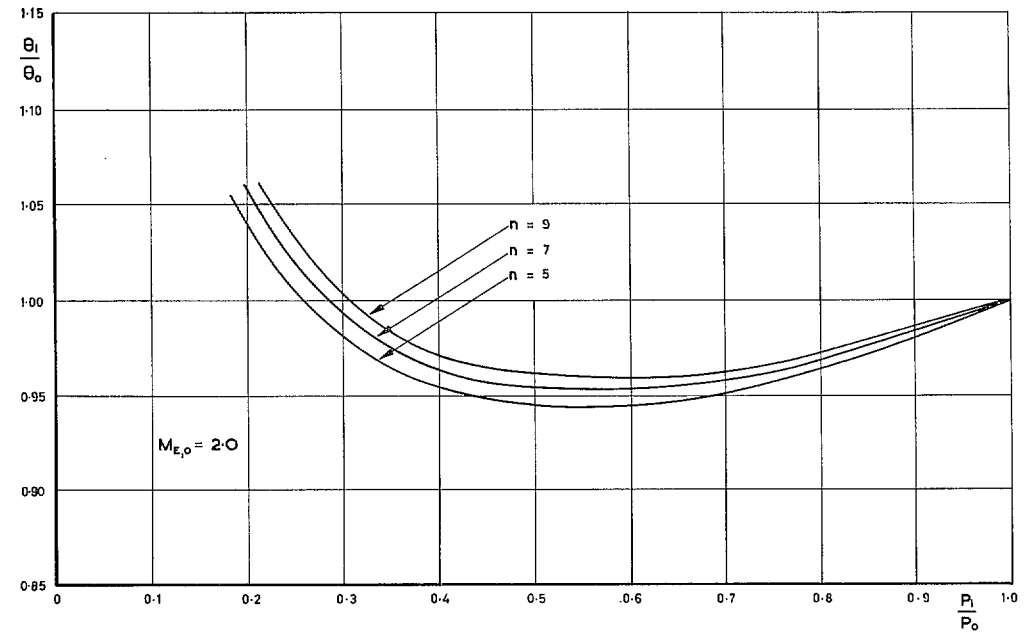

FIG. 4. Effect of abrupt expansion on boundary-layer momentum thickness—II.

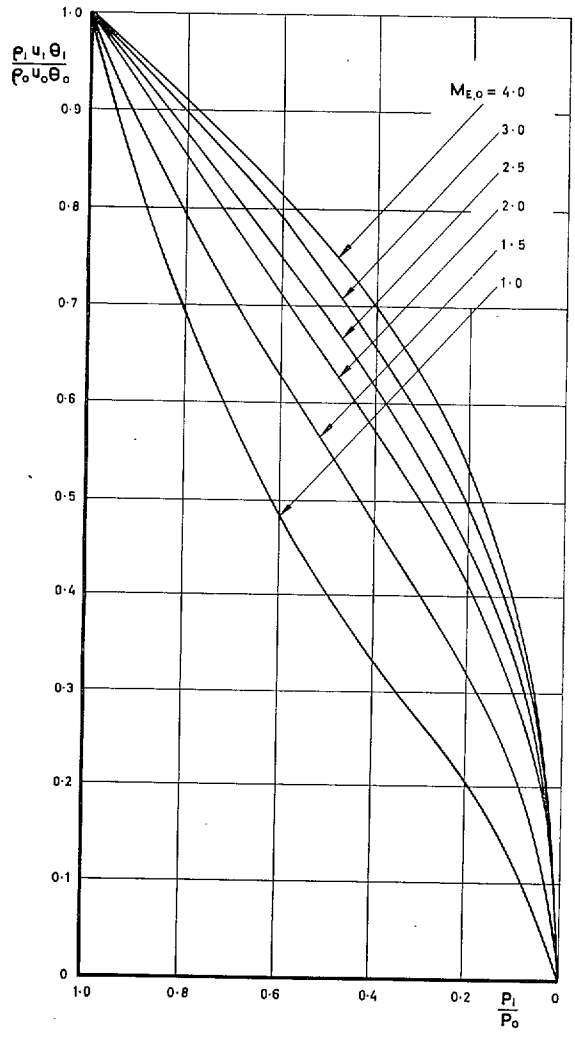

FIG. 5. Effect of abrupt expansion on boundary-layer momentum thickness—III.

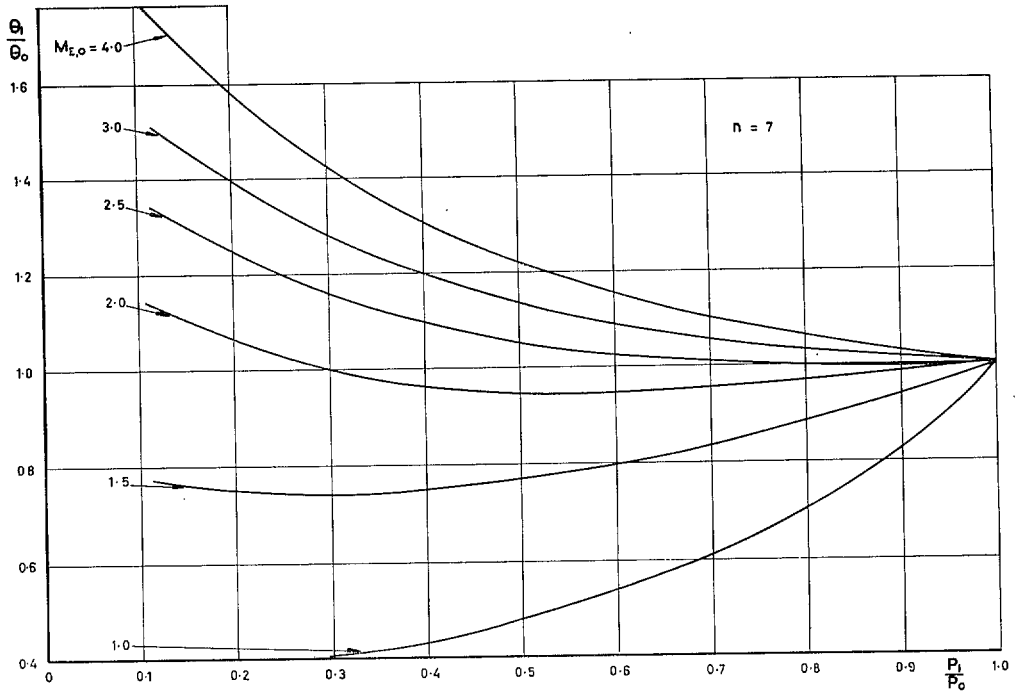

FIG. 6. Effect of abrupt expansion on boundary-layer momentum thickness—IV.

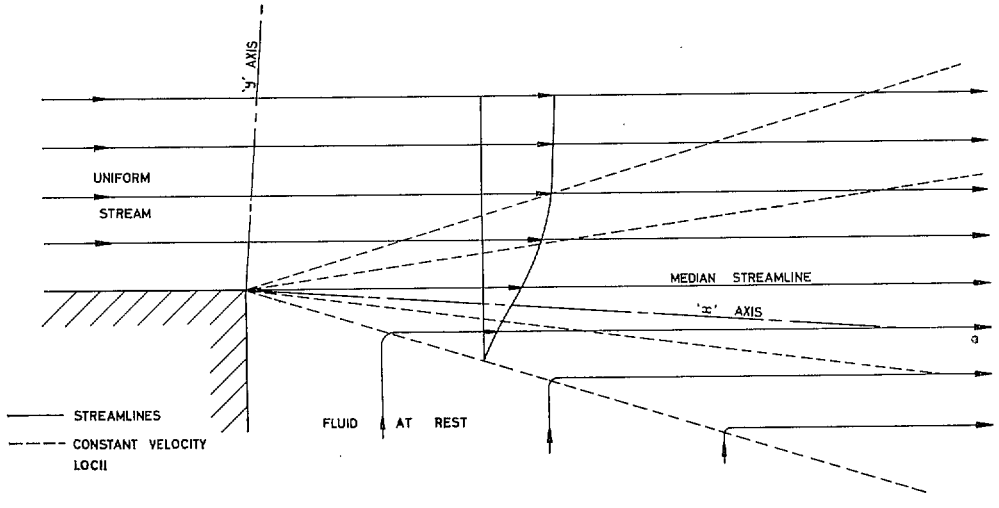

FIG. 7. The mixing of a uniform stream with a fluid at rest.

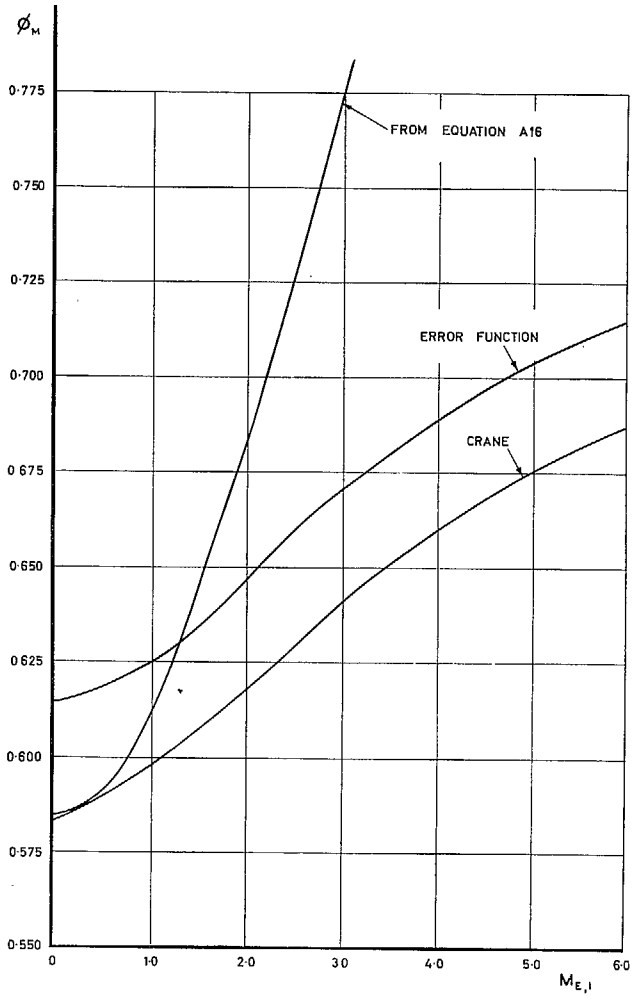

FIG. 8. Variation of ϕ_M with Mach number—I.

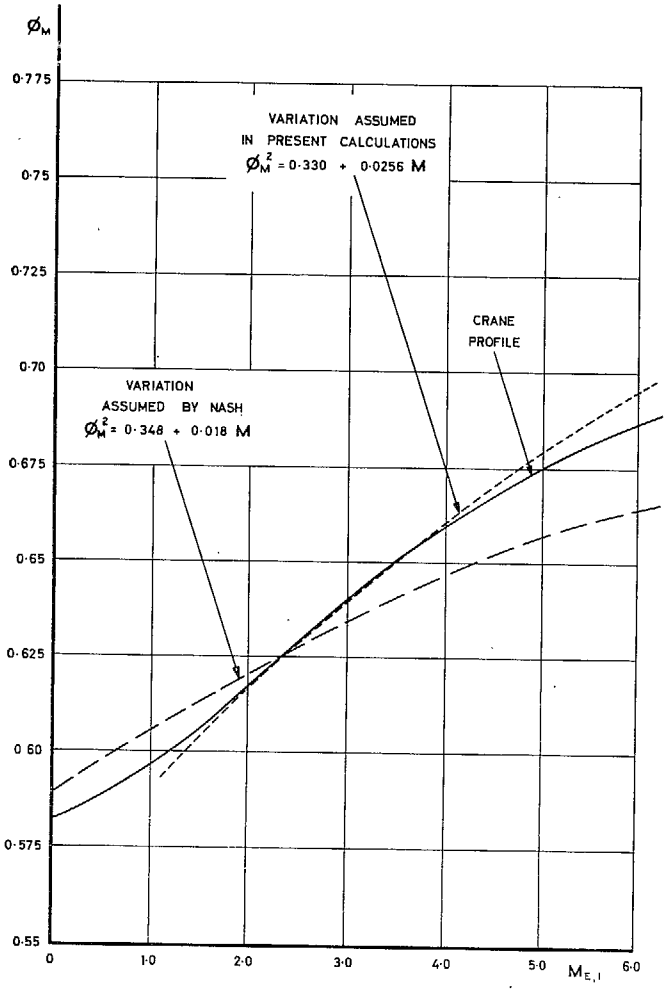

FIG. 9. Variation of ϕ_M with Mach number—II.

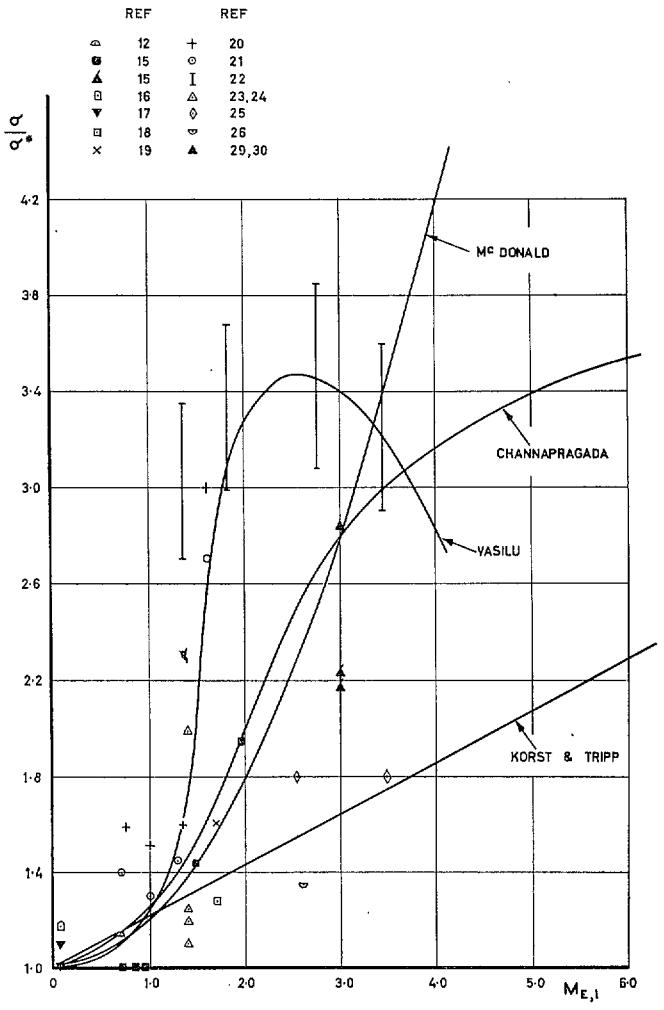

FIG. 10. Variation of σ with Mach number.

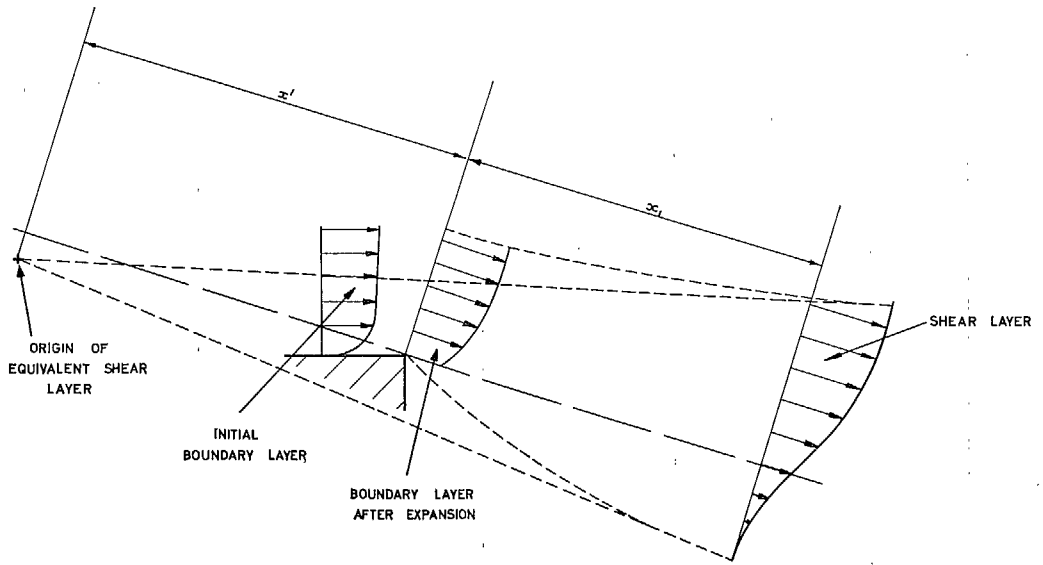

FIG. 11. Effect of initial boundary layer on the development of the shear layer.

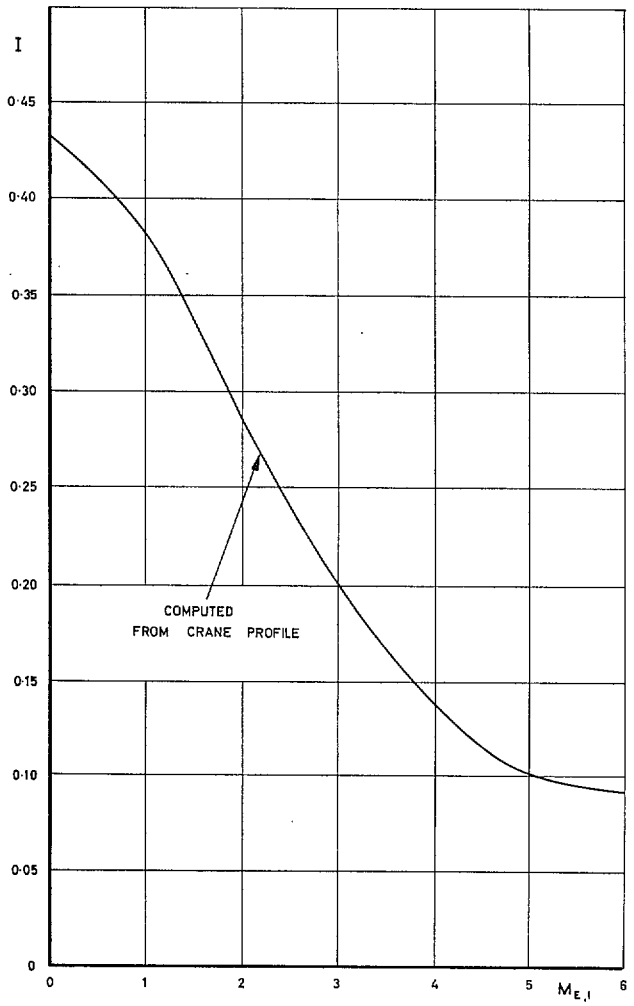

FIG. 12. Variation of I with Mach number.

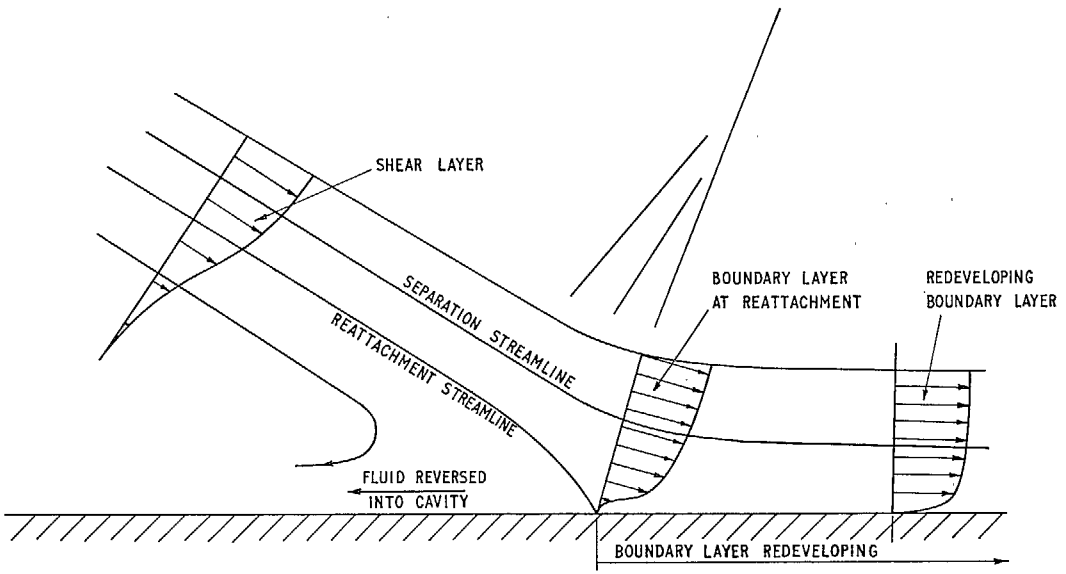

FIG. 13. Flow in the reattachment region.

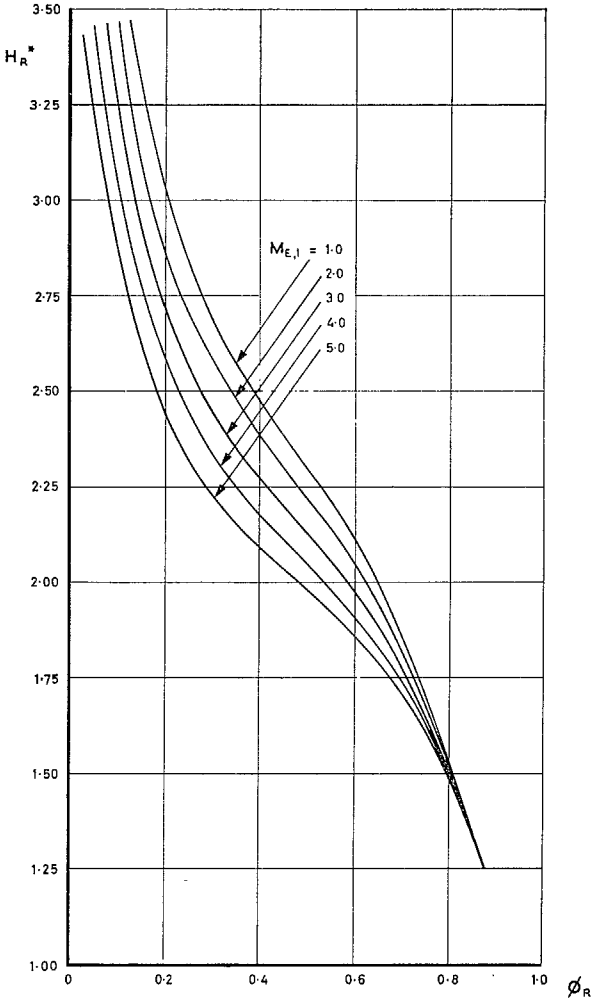

FIG. 14. Variation of H_R^* with ϕ_R.

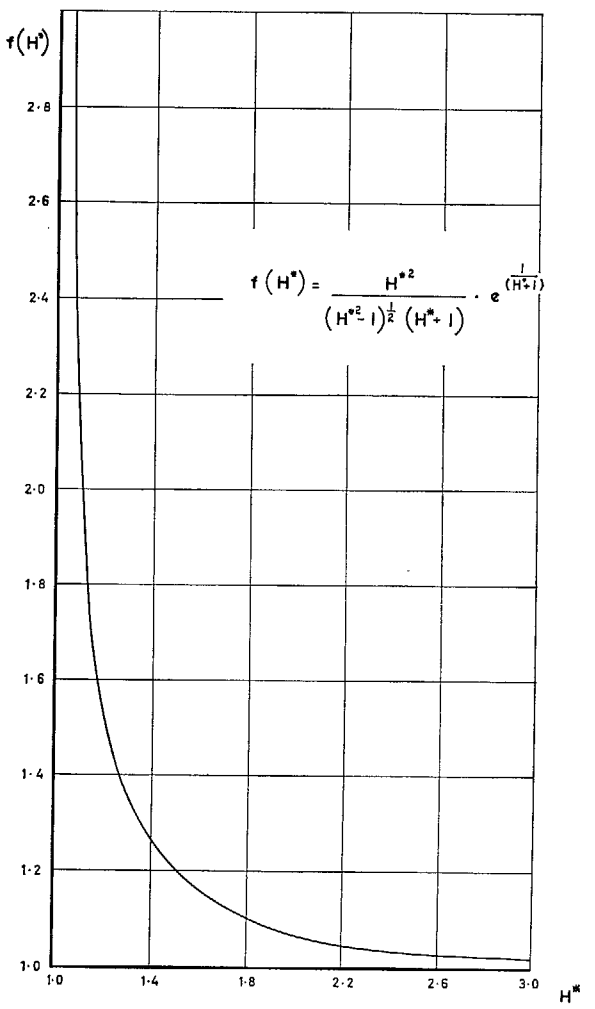

FIG. 15. Variation of $f(H^*)$ with H^*.

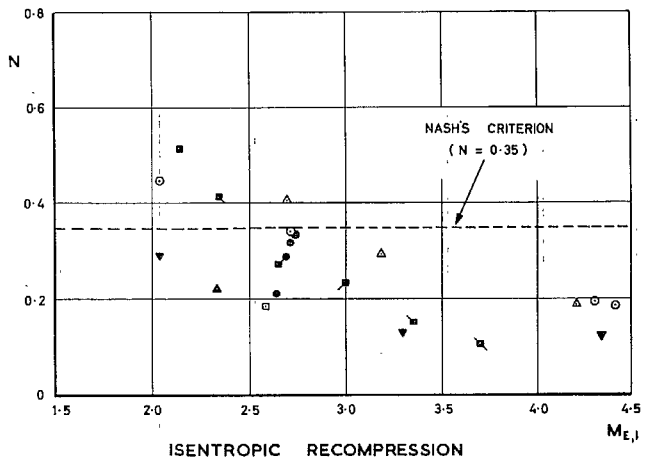

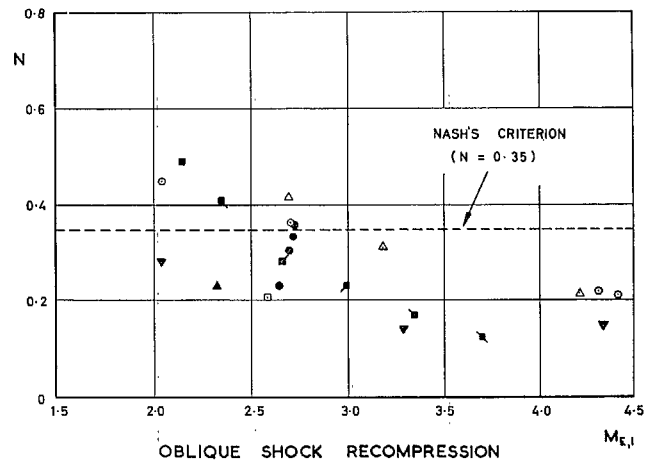

FIG. 16. Variation of N with $M_{E,1}$.

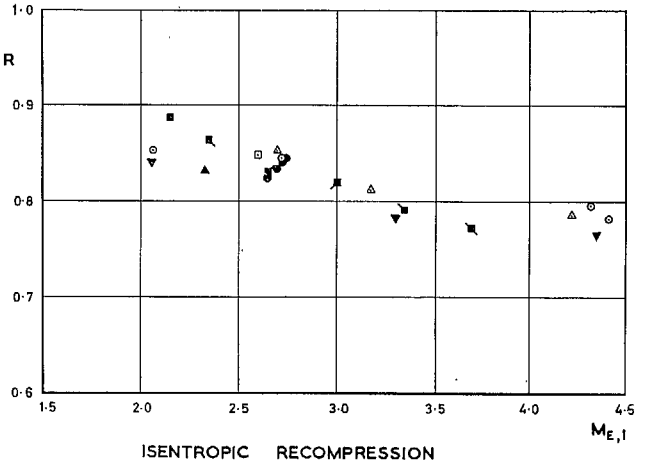

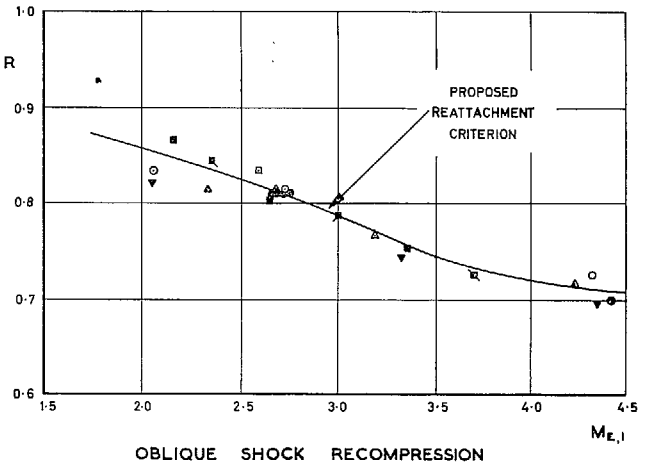

FIG. 17. Variation of R with $M_{E,1}$.

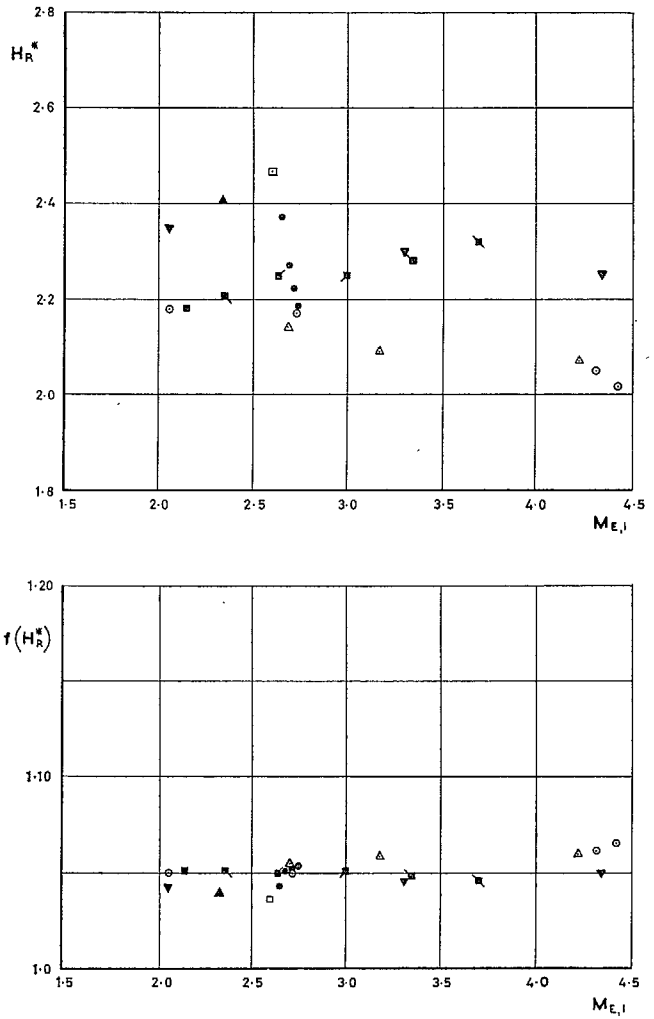

FIG. 18. Variation of H_R^* and $f(H_R^*)$ with $M_{E,1}$.

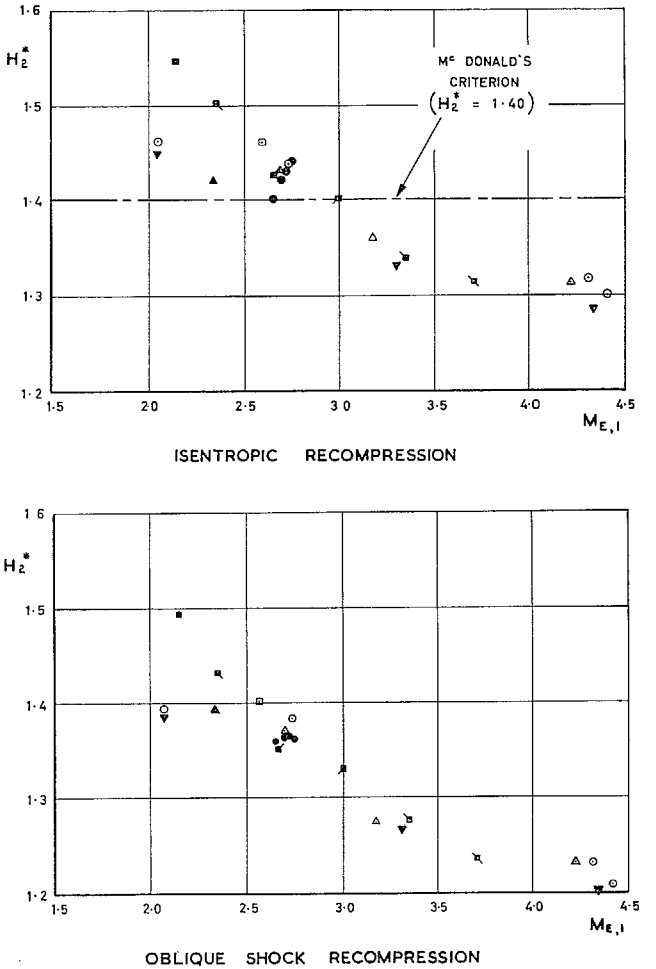

FIG. 19. Variation of H_2^* with $M_{E,1}$.

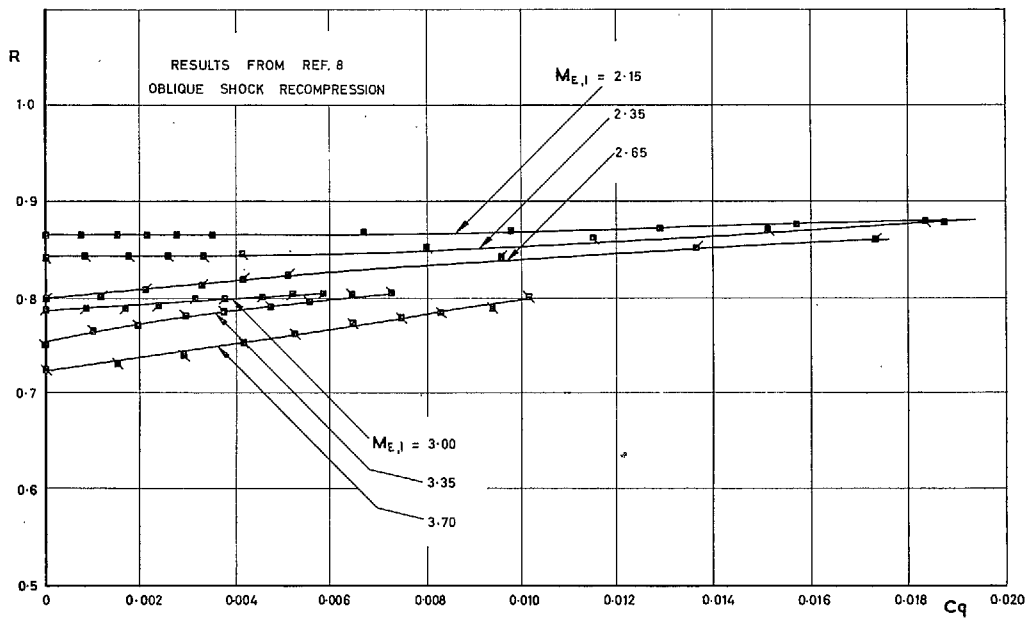

FIG. 20. Variation of R with bleed flow coefficient.

(92794) Wt. 67/7689 K 5 10/66 Hw.

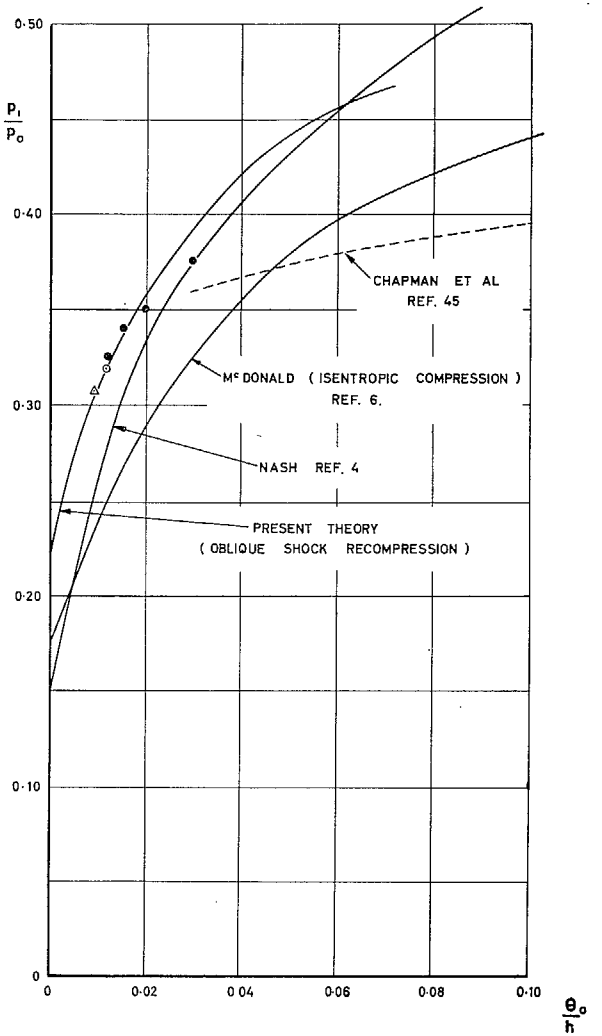

FIG. 21. Variation of base pressure with boundary-layer momentum thickness ($M_{E,0} = 2{\cdot}0$).

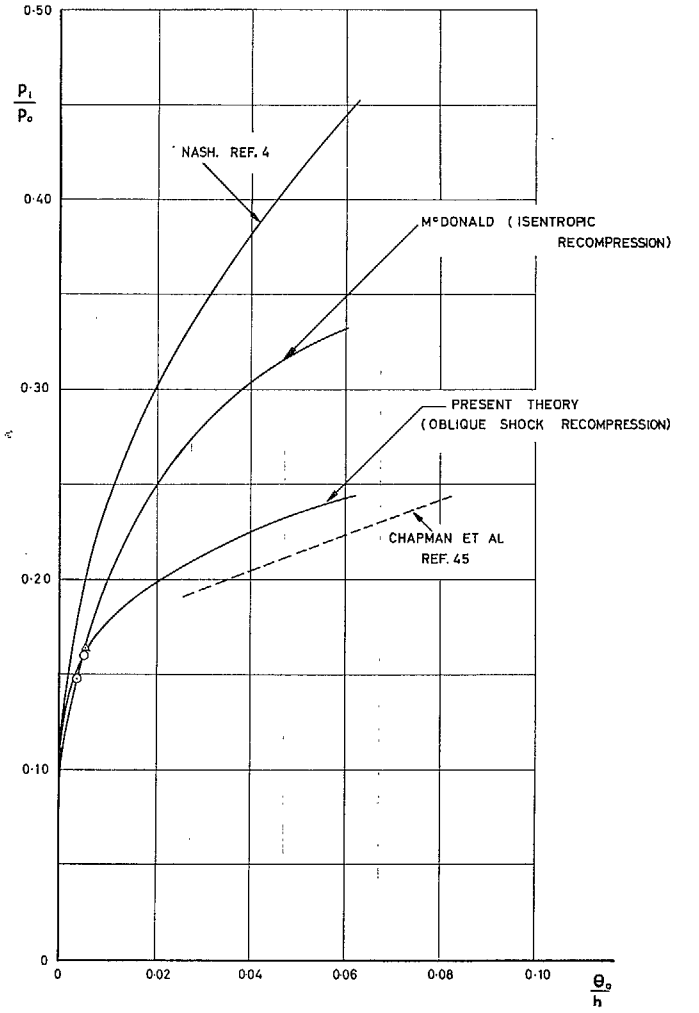

FIG. 22. Variation of base pressure with boundary-layer momentum thickness ($M_{E,0} = 3{\cdot}0$).

Printed and published by
HER MAJESTY'S STATIONERY OFFICE

To be purchased from
49 High Holborn, London WC1
423 Oxford Street, London W1
13A Castle Street, Edinburgh 2
109 St. Mary Street, Cardiff
Brazennose Street, Manchester 2
50 Fairfax Street, Bristol 1
35 Smallbrook, Ringway, Birmingham 5
80 Chichester Street, Belfast 1
or through any bookseller

Printed in England

S.O. Code No. 23-3434

Publications of the Aeronautical Research Council

ANNUAL TECHNICAL REPORTS OF THE AERONAUTICAL RESEARCH COUNCIL (BOUND VOLUMES)

1945 Vol. I. Aero and Hydrodynamics, Aerofoils. £6 10s. (£6 14s.)
Vol. II. Aircraft, Airscrews, Controls. £6 10s. (£6 14s.)
Vol. III. Flutter and Vibration, Instruments, Miscellaneous, Parachutes, Plates and Panels, Propulsion. £6 10s. (£6 14s.)
Vol. IV. Stability, Structures, Wind Tunnels, Wind Tunnel Technique. £6 10s. (£6 14s.)

1946 Vol. I. Accidents, Aerodynamics, Aerofoils and Hydrofoils. £8 8s. (£8 12s. 6d.)
Vol. II. Airscrews, Cabin Cooling, Chemical Hazards, Controls, Flames, Flutter, Helicopters, Instruments and Instrumentation, Interference, Jets, Miscellaneous, Parachutes. £8 8s. (£8 12s.)
Vol. III. Performance, Propulsion, Seaplanes, Stability, Structures, Wind Tunnels. £8 8s. (£8 12s.)

1947 Vol. I. Aerodynamics, Aerofoils, Aircraft. £8 8s. (£8 12s. 6d.)
Vol. II. Airscrews and Rotors, Controls, Flutter, Materials, Miscellaneous, Parachutes, Propulsion, Seaplanes, Stability, Structures, Take-off and Landing. £8 8s. (£8 12s. 6d.)

1948 Vol. I. Aerodynamics, Aerofoils, Aircraft, Airscrews, Controls, Flutter and Vibration, Helicopters, Instruments, Propulsion, Seaplane, Stability, Structures, Wind Tunnels. £6 10s. (£6 14s.)
Vol. II. Aerodynamics, Aerofoils, Aircraft, Airscrews, Controls, Flutter and Vibration, Helicopters, Instruments, Propulsion, Seaplane, Stability, Structures, Wind Tunnels. £5 10s. (£5 14s.)

1949 Vol. I. Aerodynamics, Aerofoils. £5 10s. (£5 14s.)
Vol. II. Aircraft, Controls, Flutter and Vibration, Helicopters, Instruments, Materials, Seaplanes, Structures, Wind Tunnels. £5 10s. (£5 13s. 6d.)

1950 Vol. I. Aerodynamics, Aerofoils, Aircraft. £5 12s. 6d. (£5 16s. 6d.)
Vol. II. Apparatus, Flutter and Vibration, Meteorology, Panels, Performance, Rotorcraft, Seaplanes. £4 (£4 3s. 6d.)
Vol. III. Stability and Control, Structures, Thermodynamics, Visual Aids, Wind Tunnels. £4 (£4 3s. 6d.)

1951 Vol. I. Aerodynamics, Aerofoils. £6 10s. (£6 14s.)
Vol. II. Compressors and Turbines, Flutter, Instruments, Mathematics, Ropes, Rotorcraft, Stability and Control, Structures, Wind Tunnels. £5 10s. (£5 14s.)

1952 Vol. I. Aerodynamics, Aerofoils. £8 8s. (£8 12s.)
Vol. II. Aircraft, Bodies, Compressors, Controls, Equipment, Flutter and Oscillation, Rotorcraft, Seaplanes, Structures. £5 10s. (£5 13s. 6d.)

1953 Vol. I. Aerodynamics, Aerofoils and Wings, Aircraft, Compressors and Turbines, Controls. £6 (£6 4s.)
Vol. II. Flutter and Oscillation, Gusts, Helicopters, Performance, Seaplanes, Stability, Structures, Thermodynamics, Turbulence. £5 5s. (£5 9s.)

1954 Aero and Hydrodynamics, Aerofoils, Arrester gear, Compressors and Turbines, Flutter, Materials, Performance, Rotorcraft, Stability and Control, Structures. £7 7s. (£7 11s.)

Special Volumes

Vol. I. Aero and Hydrodynamics, Aerofoils, Controls, Flutter, Kites, Parachutes, Performance, Propulsion, Stability. £6 6s. (£6 9s. 6d.)
Vol. II. Aero and Hydrodynamics, Aerofoils, Airscrews, Controls, Flutter, Materials, Miscellaneous, Parachutes, Propulsion, Stability, Structures. £7 7s. (£7 10s. 6d.)
Vol. III. Aero and Hydrodynamics, Aerofoils, Airscrews, Controls, Flutter, Kites, Miscellaneous, Parachutes, Propulsion, Seaplanes, Stability, Structures, Test Equipment. £9 9s. (£9 13s. 6d.)

Reviews of the Aeronautical Research Council

1949–54 5s. (5s. 6d.)

Index to all Reports and Memoranda published in the Annual Technical Reports

1909–1947 R. & M. 2600 (out of print)

Indexes to the Reports and Memoranda of the Aeronautical Research Council

Between Nos. 2451–2549: R. & M. No. 2550 2s. 6d. (2s. 9d.); Between Nos. 2651–2749: R. & M. No. 2750 2s. 6d. (2s. 9d.); Between Nos. 2751–2849: R. & M. No. 2850 2s. 6d. (2s. 9d.); Between Nos. 2851–2949: R. & M. No. 2950 3s. (3s. 3d.); Between Nos. 2951–3049: R. & M. No. 3050 3s. 6d. (3s. 9d.); Between Nos. 3051–3149: R. & M. No. 3150 3s. 6d. (3s. 9d.); Between Nos. 3151–3249: R. & M. No. 3250 3s. 6d. (3s. 9d.); Between Nos. 3251–3349: R. & M. No. 3350 3s. 6d. (3s. 11d.)

Prices in brackets include postage

Government publications can be purchased over the counter or by post from the Government Bookshops in London, Edinburgh, Cardiff, Belfast, Manchester, Birmingham and Bristol, or through any bookseller